

RECEIVED: July 3, 2014

REVISED: August 18, 2014

ACCEPTED: September 1, 2014

PUBLISHED: October 7, 2014

CP violation with a dynamical Higgs

M.B. Gavela,^a J. Gonzalez-Fraile,^b M.C. Gonzalez-Garcia,^{b,c,d} L. Merlo,^a S. Rigolin^e
and J. Yepes^a

^a*Departamento de Física Teórica and Instituto de Física Teórica,
IFT-UAM/CSIC, Universidad Autónoma de Madrid,
Cantoblanco, 28049, Madrid, Spain*

^b*Departament d'Estructura i Constituents de la Matèria and ICC-UB, Universitat de Barcelona,
647 Diagonal, E-08028 Barcelona, Spain*

^c*C.N. Yang Institute for Theoretical Physics and
Department of Physics and Astronomy, SUNY at Stony Brook,
Stony Brook, NY 11794-3840, U.S.A.*

^d*Institució Catalana de Recerca i Estudis Avançats (ICREA),
Barcelona, Spain*

^e*Dipartimento di Fisica e Astronomia "G. Galilei", Università di Padova and
INFN, Sezione di Padova,
Via Marzolo 8, I-35131 Padua, Italy*

E-mail: belen.gavela@uam.es, fraile@ecm.ub.edu,
concha@insti.physics.sunysb.edu, luca.merlo@uam.es,
stefano.rigolin@pd.infn.it, ju.yepes@uam.es

ABSTRACT: We determine the complete set of independent gauge and gauge-Higgs CP-odd effective operators for the generic case of a dynamical Higgs, up to four derivatives in the chiral expansion. The relation with the linear basis of dimension six CP-odd operators is clarified. Phenomenological applications include bounds inferred from electric dipole moment limits, and from present and future collider data on triple gauge coupling measurements and Higgs signals.

KEYWORDS: Higgs Physics, Beyond Standard Model, CP violation, Technicolor and Composite Models

ARXIV EPRINT: [1406.6367](https://arxiv.org/abs/1406.6367)

Contents

1	Introduction	1
2	Effective CP-odd chiral bosonic Lagrangian	2
2.1	Basis of CP-odd pure gauge and gauge-Higgs operators	4
3	Phenomenology	5
3.1	CP-odd two-point functions	5
3.2	Triple gauge boson couplings	7
3.2.1	CP violation in $WW\gamma$: fermionic EDMs	8
3.2.2	CP violation in WWZ : collider bounds and signatures	10
3.3	CP violation in Higgs couplings to gauge-boson pairs	15
4	Conclusions	18
A	Linear siblings of chiral operators	20
B	Feynman rules	21

1 Introduction

While charge conjugation (C) and parity (P) are not exact symmetries of the Standard Model of particle physics, present data [1–4] are consistent with the Higgs particle being the Standard Model (SM) scalar [5–7], which is defined as a CP-even $SU(2)_L$ doublet scalar. Nevertheless, in the plausible perspective that particle physics is not at the end of the road and beyond the SM physics (BSM) is awaiting discovery as an explanation of the electroweak hierarchy problem, it is necessary to track the possible non-doublet and/or CP-odd components of the observed resonance, in particular in view of the sizeable present error bars. This is underway through different complementary strategies: kinematical analysis, direct searches of new resonances expected in particular BSM theories, or indirect signals other than kinematic ones. Indirect searches may well give fruitful results prior to the discovery of new resonances, and may allow to explore and disentangle the two possible avenues of realisation of electroweak symmetry breaking (EWSB): linear [8–44] –which is typical of BSM theories in which the Higgs particle is elementary– or non-linear [45–55] –as for instance in models in which the Higgs boson is a composite pseudo-goldstone boson of some strong-interacting BSM theory or a dilaton.

Interesting past and new proposals to search for CP-odd anomalous couplings of the Higgs boson to fermions and gauge bosons [35, 56–91] rank from purely phenomenological analysis to the identification of effective signals expected assuming either a linear or a

non-linear realisation of EWSB. In previous literature, some of the CP-odd gauge and/or gauge-Higgs operators to be discussed below had not been explored, but traded instead by fermionic ones via the equations of motion.¹ Nevertheless, it is theoretically very interesting to identify and analyse the complete set of independent CP-odd bosonic operators, as they may shed a direct light on the nature of EWSB, which takes place precisely in the bosonic sector. Moreover, the present LHC data offer increasingly rich and precise constraints on gauge and gauge-Higgs couplings, up to the point of becoming competitive with fermionic bounds in constraining BSM theories; this trend may be further strengthened with the post-LHC facilities presently under discussion.

We discuss here the issue of CP-violation in the case of non-linear realisations of EWSB. To be generic and model-independent, a non-linear (also dubbed “chiral”) effective Lagrangian will be used to describe physics at energies lower than the characteristic BSM scale(s). The complete and independent set — that is, the basis — of CP-odd bosonic operators of the non-linear expansion will be determined here for the first time, up to four derivative couplings. The differences with the leading anomalous couplings and signals expected from linear realizations of BSM physics will be also identified. Phenomenological constraints resulting from limits on electric dipole moments (EDMs) and from present LHC data will be derived as well, and future prospects briefly discussed. The structure of the paper can be easily inferred from the table of Contents.

2 Effective CP-odd chiral bosonic Lagrangian

Reference [51] developed the effective Lagrangian for a light dynamical Higgs, up to four derivative couplings and restricted to the CP-even bosonic sector except for the inclusion of Yukawa-like interactions.² Its CP-odd counterpart will be studied below.

The most up-to-date analyses of Higgs data have established that the couplings of h to the gauge bosons and the absolute values of its couplings to fermions are compatible with the SM ones.³ It is then justified from the phenomenological point of view to consider the SM as the leading-order Lagrangian \mathcal{L}_{SM} and treat as corrections all possible departures due to the unknown high-energy strong dynamics. Here only the CP-odd sector will be explicitly addressed, while the CP-even sector has been already studied in refs. [51] and will be left implicit. The effective Lagrangian can then be written as

$$\mathcal{L}_{\text{chiral}} = \mathcal{L}_{SM} + \Delta\mathcal{L}_{\text{CP}}, \quad (2.1)$$

¹See for instance ref. [53] for an analysis in the framework of non-linear EWSB.

²As usual, derivative is understood in the sense of covariant derivative. That is, a gauge field and a momentum have both chiral dimension one and their inclusion in non-renormalizable operators is weighted down by the same high-energy strong-interaction scale Λ_s .

³The sign of the couplings between h and fermions is still to be measured, although a slight preference for a positive value is indicated in some two parameter fits (see for example [18, 19, 28]) which take into account one-loop induced EW corrections; we will consider this option in what follows.

where the first term reads

$$\begin{aligned}
 \mathcal{L}_{SM} = & \frac{1}{2}(\partial_\mu h)(\partial^\mu h) - \frac{1}{4}B_{\mu\nu}B^{\mu\nu} - \frac{1}{4}W_{\mu\nu}^a W^{a\mu\nu} - \frac{1}{4}G_{\mu\nu}^a G^{a\mu\nu} - V(h) \\
 & - \frac{(v+h)^2}{4}\text{Tr}[\mathbf{V}_\mu \mathbf{V}^\mu] + i\bar{Q}\not{D}Q + i\bar{L}\not{D}L \\
 & - \frac{v+h}{\sqrt{2}}(\bar{Q}_L \mathbf{U} \mathbf{Y}_Q Q_R + \text{h.c.}) - \frac{v+h}{\sqrt{2}}(\bar{L}_L \mathbf{U} \mathbf{Y}_L L_R + \text{h.c.}) \\
 & - \frac{g_s^2}{16\pi^2}\theta_s G_{\mu\nu}^a \tilde{G}_{\rho\sigma}^a.
 \end{aligned} \tag{2.2}$$

In this expression $\mathbf{U} \equiv \exp(i\pi \cdot \tau/v)$ –with τ denoting the Pauli matrices– is a unitary matrix which efficiently encodes the longitudinal degrees of freedom of the heavy gauge bosons and transforms as a $(2,2)$ of the global $\text{SU}(2)_L \times \text{SU}(2)_R$ symmetry group of the Lagrangian, and $\mathbf{V}_\mu \equiv (\mathbf{D}_\mu \mathbf{U}) \mathbf{U}^\dagger$ is the vector chiral field transforming in the adjoint of $\text{SU}(2)_L$. Furthermore, v is the EW scale, defined via the W gauge boson mass $M_W = gv/2$, and h denotes the Higgs particle. The covariant derivative reads

$$\mathbf{D}_\mu \mathbf{U}(x) \equiv \partial_\mu \mathbf{U}(x) + igW_\mu(x)\mathbf{U}(x) - \frac{ig'}{2}B_\mu(x)\mathbf{U}(x)\tau_3, \tag{2.3}$$

with $W_\mu \equiv W_\mu^a(x)\tau_a/2$ and B_μ denoting the $\text{SU}(2)_L$ and $\text{U}(1)_Y$ gauge bosons, respectively. In eq. (2.2), the first line describes the h and gauge boson kinetic terms, as well as the effective scalar potential $V(h)$, accounting for the breaking of the electroweak symmetry. The second line describes the W and Z masses and their interactions with h , as well as the kinetic terms for Goldstone bosons and fermions. The third line corresponds to the Yukawa-like interactions written in the fermionic mass eigenstate basis. A compact notation for the right-handed fields has been adopted, gathering them into doublets Q_R and L_R . \mathbf{Y}_Q and \mathbf{Y}_L are two 6×6 block-diagonal matrices containing the usual Yukawa couplings:

$$\mathbf{Y}_Q \equiv \text{diag}(Y_U, Y_D), \quad \mathbf{Y}_L \equiv \text{diag}(Y_\nu, Y_L), \tag{2.4}$$

where the Cabibbo-Kobayashi-Maskawa mixing is understood to be encoded in the definition of Q_L , thus accounting for the SM CP-even fermionic couplings. Finally, the last term in eq. (2.2) corresponds to the well-known total derivative CP-odd gluonic coupling, for which the notation used is that in which the dual field-tensor of any field strength $X_{\mu\nu}$ is defined as $\tilde{X}^{\mu\nu} \equiv \frac{1}{2}\epsilon^{\mu\nu\rho\sigma}X_{\rho\sigma}$.

This description is data-driven and, while being a consistent chiral expansion up to four derivatives, the particular division in eq. (2.1) does not match that in number of derivatives, usually adopted by chiral Lagrangian practitioners. For instance, the usual custodial breaking term $\text{Tr}(\mathbf{T}\mathbf{V}_\mu)\text{Tr}(\mathbf{T}\mathbf{V}^\mu)$, being $\mathbf{T} \equiv \mathbf{U}\tau_3\mathbf{U}^\dagger$, is a two derivative operator and is often listed among the leading order set in the chiral expansion; however, it is not present in the SM at tree level and data strongly constrain its coefficient so that in practice it can be always considered [49] a subleading operator. Moreover, in the phenomenological Lagrangian in eq. (2.2) the Higgs couplings with gauge bosons and fermions have been taken SM-like, as suggested by data. However, in the non-linearly realized EWSB framework, this is not guaranteed by any symmetry and it should be considered as a phenomenological

accident. A more general notation has been adopted in ref. [51] for the case of the CP-even chiral Lagrangian for a dynamical Higgs. This issue is irrelevant for the focus of this paper, as if the latter notation was adopted here, the complete four-derivative basis $\Delta\mathcal{L}_{\mathcal{CP}}$ (see below eq. (2.6)) would be exactly the same.

2.1 Basis of CP-odd pure gauge and gauge-Higgs operators

The CP-odd corrections will be parametrised as

$$\Delta\mathcal{L}_{\mathcal{CP}} = c_{\tilde{B}} \mathcal{S}_{\tilde{B}}(h) + c_{\tilde{W}} \mathcal{S}_{\tilde{W}}(h) + c_{\tilde{G}} \mathcal{S}_{\tilde{G}}(h) + c_{2D} \mathcal{S}_{2D}(h) + \sum_{i=1}^{16} c_i \mathcal{S}_i(h), \quad (2.5)$$

where c_i are model-dependent constant coefficients and

$$\begin{aligned} \mathcal{S}_{\tilde{B}}(h) &\equiv -\frac{1}{2}g'^2 B^{\mu\nu} \tilde{B}_{\mu\nu} \mathcal{F}_{\tilde{B}}(h), & \mathcal{S}_7(h) &\equiv g \text{Tr}(\mathbf{T} [W^{\mu\nu}, \mathbf{V}_\mu]) \partial_\nu \mathcal{F}_7(h), \\ \mathcal{S}_{\tilde{W}}(h) &\equiv -\frac{1}{2}g^2 \text{Tr}(W^{\mu\nu} \tilde{W}_{\mu\nu}) \mathcal{F}_{\tilde{W}}(h), & \mathcal{S}_8(h) &\equiv 2g^2 \text{Tr}(\mathbf{T} \tilde{W}^{\mu\nu}) \text{Tr}(\mathbf{T} W_{\mu\nu}) \mathcal{F}_8(h), \\ \mathcal{S}_{\tilde{G}}(h) &\equiv -\frac{1}{2}g_s^2 G^{a\mu\nu} \tilde{G}_{\mu\nu}^a \mathcal{F}_{\tilde{G}}(h), & \mathcal{S}_9(h) &\equiv 2ig \text{Tr}(\tilde{W}^{\mu\nu} \mathbf{T}) \text{Tr}(\mathbf{T} \mathbf{V}_\mu) \partial_\nu \mathcal{F}_9(h), \\ \mathcal{S}_{2D}(h) &\equiv i \frac{v^2}{4} \text{Tr}(\mathbf{T} \mathcal{D}^\mu \mathbf{V}_\mu) \mathcal{F}_{2D}(h), & \mathcal{S}_{10}(h) &\equiv i \text{Tr}(\mathbf{V}^\mu \mathcal{D}^\nu \mathbf{V}_\nu) \text{Tr}(\mathbf{T} \mathbf{V}_\mu) \mathcal{F}_{10}(h), \\ \mathcal{S}_1(h) &\equiv 2gg' \tilde{B}^{\mu\nu} \text{Tr}(\mathbf{T} W_{\mu\nu}) \mathcal{F}_1(h), & \mathcal{S}_{11}(h) &\equiv i \text{Tr}(\mathbf{T} \mathcal{D}^\mu \mathbf{V}_\mu) \text{Tr}(\mathbf{V}^\nu \mathbf{V}_\nu) \mathcal{F}_{11}(h), \\ \mathcal{S}_2(h) &\equiv 2ig' \tilde{B}^{\mu\nu} \text{Tr}(\mathbf{T} \mathbf{V}_\mu) \partial_\nu \mathcal{F}_2(h), & \mathcal{S}_{12}(h) &\equiv i \text{Tr}([\mathbf{V}^\mu, \mathbf{T}] \mathcal{D}^\nu \mathbf{V}_\nu) \partial_\mu \mathcal{F}_{12}(h), \\ \mathcal{S}_3(h) &\equiv 2ig \text{Tr}(\tilde{W}^{\mu\nu} \mathbf{V}_\mu) \partial_\nu \mathcal{F}_3(h), & \mathcal{S}_{13}(h) &\equiv i \text{Tr}(\mathbf{T} \mathcal{D}^\mu \mathbf{V}_\mu) \partial^\nu \partial_\nu \mathcal{F}_{13}(h), \\ \mathcal{S}_4(h) &\equiv g \text{Tr}(W^{\mu\nu} \mathbf{V}_\mu) \text{Tr}(\mathbf{T} \mathbf{V}_\nu) \mathcal{F}_4(h), & \mathcal{S}_{14}(h) &\equiv i \text{Tr}(\mathbf{T} \mathcal{D}^\mu \mathbf{V}_\mu) \partial^\nu \mathcal{F}_{14}(h) \partial_\nu \mathcal{F}'_{14}(h), \\ \mathcal{S}_5(h) &\equiv i \text{Tr}(\mathbf{V}^\mu \mathbf{V}^\nu) \text{Tr}(\mathbf{T} \mathbf{V}_\mu) \partial_\nu \mathcal{F}_5(h), & \mathcal{S}_{15}(h) &\equiv i \text{Tr}(\mathbf{T} \mathbf{V}^\mu) (\text{Tr}(\mathbf{T} \mathbf{V}^\nu))^2 \partial_\mu \mathcal{F}_{15}(h), \\ \mathcal{S}_6(h) &\equiv i \text{Tr}(\mathbf{V}^\mu \mathbf{V}_\mu) \text{Tr}(\mathbf{T} \mathbf{V}^\nu) \partial_\nu \mathcal{F}_6(h), & \mathcal{S}_{16}(h) &\equiv i \text{Tr}(\mathbf{T} \mathcal{D}^\mu \mathbf{V}_\mu) (\text{Tr}(\mathbf{T} \mathbf{V}^\nu))^2 \mathcal{F}_{16}(h), \end{aligned} \quad (2.6)$$

with the $\mathcal{F}_i(h)$ -functions for all operators⁴ but $\mathcal{S}_{\tilde{G}}(h)$ being generic functions of the scalar singlet h defined as [51]

$$\mathcal{F}_i(h) \equiv 1 + 2a_i \frac{h}{v} + b_i \frac{h^2}{v^2} + \dots, \quad (2.7)$$

with dots standing for terms with higher powers in h/v which will not be considered below. $\mathcal{F}_{\tilde{G}}(h)$ will be understood to be also of this form but for the first term in eq. (2.7), as the Higgs-independent part of $\mathcal{S}_{\tilde{G}}(h)$ has already been included in the SM Lagrangian, eq. (2.2).

The Lagrangian in eqs. (2.1) and (2.5) describes the CP-odd low-energy effects of a high-energy strong dynamics responsible for the electroweak GBs, coupled to a generic scalar singlet h . Note that the number of independent operators in the non-linear expansion turned out to be larger than for the analogous basis in the linear expansion [54, 55], a generic feature when comparing both type of effective Lagrangians; see appendix A. The basis is also larger than that for chiral expansions developed in the past for the case of a very heavy

⁴The Higgs-independent term in this functional is physically irrelevant for operators $\mathcal{S}_{\tilde{B}}(h)$, $\mathcal{S}_{\tilde{W}}(h)$, $\mathcal{S}_{2D}(h)$.

Higgs particle (i.e. absent at low energies) [92–95], as: i) terms which in the absence of the $\mathcal{F}_i(h)$ functions were shown to be equivalent via total derivatives, are now independent; ii) new terms including derivatives of h appear.

3 Phenomenology

In what follows we analyse the physical impact of the operators in the CP-odd bosonic basis determined above. Some phenomenological bounds and future prospects are discussed as well.

3.1 CP-odd two-point functions

Only the operators $\mathcal{S}_{2D}(h)$ and $\mathcal{S}_{13}(h)$ among those defined in eq. (2.6) may a priori induce renormalisation effects on the fields and couplings of the SM Lagrangian. $\mathcal{S}_{2D}(h)$ is a two-derivative coupling and thus part of the leading order of the chiral expansion; in contrast, note that it has no analogue in the leading order ($d = 4$) of the linear expansion –in other words in the SM Lagrangian– as its lower-dimensional linear sibling would be a dimension six ($d = 6$) operator, see appendix A.

$\mathcal{S}_{2D}(h)$ and $\mathcal{S}_{13}(h)$ contain two-point functions which explicitly break the CP symmetry and as a consequence the Lagrangian eigenstates may not be CP-eigenstates. Those two couplings result in a mixing of h with the Goldstone bosons which in the SM give masses to the W and Z bosons, see below. Their physical impact reduces simply to anomalous CP-odd Higgs-fermion and Higgs- Z couplings, as we show next in detail.

Consider the linear combination of the two operators $\mathcal{S}_{2D}(h)$ and $\mathcal{S}_{13}(h)$, together with the h -kinetic term and the gauge-boson mass term in the Lagrangian of eq. (2.1), and let us focus first on their contribution to two-point functions:

$$\begin{aligned} \mathcal{L}_{\text{chiral}} \supset & \frac{1}{2} \partial^\mu h \partial_\mu h - \frac{(v+h)^2}{4} \text{Tr}(\mathbf{V}^\mu \mathbf{V}_\mu) + c_{2D} \mathcal{S}_{2D}(h) + c_{13} \mathcal{S}_{13}(h) \\ & \supset \frac{1}{2} \partial^\mu h \partial_\mu h + \frac{v^2}{4} \text{Tr}(\partial^\mu \mathbf{U}^\dagger \partial_\mu \mathbf{U}) + \frac{i}{2} v \text{Tr}(\mathbf{T} (\partial_\mu \partial^\mu \mathbf{U}) \mathbf{U}^\dagger) (\hat{a}_{2D} h + \frac{4}{v^2} \hat{a}_{13} \square h) + \\ & + \frac{i}{2} g' B^\mu \left\{ \frac{v^2}{4} \text{Tr} \left((\partial_\mu \mathbf{U}) \tau_3 \mathbf{U}^\dagger - \mathbf{U} \tau_3 (\partial_\mu \mathbf{U}^\dagger) \right) + i v \left[\hat{a}_{2D} \partial_\mu h + \frac{4}{v^2} \hat{a}_{13} \partial_\mu (\square h) \right] \right\} \\ & + \frac{i}{2} g W_\mu^i \left\{ \frac{v^2}{4} \text{Tr} \left((\partial^\mu \mathbf{U}^\dagger) \tau^i \mathbf{U} - \mathbf{U}^\dagger \tau^i (\partial^\mu \mathbf{U}) \right) - \frac{i v}{2} \left[\hat{a}_{2D} \partial_\mu h + \frac{4}{v^2} \hat{a}_{13} \partial_\mu (\square h) \right] \text{Tr}(\mathbf{T} \tau^i) \right\}, \end{aligned} \quad (3.1)$$

where for simplicity the definitions

$$\hat{a}_i \equiv c_i a_i \quad (3.2)$$

have been implemented, with c_i being the operator coefficients in eq. (2.5) and a_i the coefficients of the terms linear in the Higgs field in eq. (2.7).

In what concerns the Lagrangian two-point functions, the dependence on \hat{a}_{2D} and \hat{a}_{13} in eq. (3.1) can be reabsorbed via a phase redefinition of the Goldstone boson \mathbf{U} matrix in eq. (2.2) of the form

$$\mathbf{U} = \tilde{\mathbf{U}} \exp \left[-\frac{i}{v} \left(\hat{a}_{2D} h + 4 \hat{a}_{13} \frac{\square h}{v^2} \right) \tau_3 \right], \quad (3.3)$$

at first order in the \hat{a}_i coefficients. This redefinition is a non-linear version of the simple Higgs-field redefinition proposed in ref. [96] when analysing the effective linear axion Lagrangian. $\tilde{\mathbf{U}}$ is then the resulting physical matrix of the Goldstone bosons eaten by the W and Z bosons, to be identified with the identity in the unitary gauge. The gauge-fixing terms can now be written in the standard form,

$$\begin{aligned}\mathcal{L}_B^{\text{GF}} &= -\frac{1}{4\eta} \text{Tr} \left(\left[\partial_\mu B^\mu - \frac{i}{4} \eta g' v^2 \left(\tilde{\mathbf{U}} \tau_3 - \tau_3 \tilde{\mathbf{U}}^\dagger \right) \right]^2 \right) \\ \mathcal{L}_W^{\text{GF}} &= -\frac{1}{\eta} \text{Tr} \left(\left[\partial_\mu W^\mu + \frac{i}{8} \eta g v^2 \left(\tilde{\mathbf{U}} - \tilde{\mathbf{U}}^\dagger \right) \right]^2 \right),\end{aligned}\tag{3.4}$$

removing all mixed gauge boson-Goldstone bosons and gauge boson- h two-point couplings.

After the redefinition in eq. (3.3) and at first order on the operator coefficients, the SM Lagrangian eq. (2.2) gets physical corrections given by

$$\Delta \mathcal{L}_{\text{Yuk}} + \Delta \mathcal{L}_{\text{Bos}},\tag{3.5}$$

with

$$\Delta \mathcal{L}_{\text{Yuk}} = \frac{i}{v} \left(\hat{a}_{2D} h + 4 \hat{a}_{13} \frac{\square h}{v^2} \right) \frac{(v+h)}{\sqrt{2}} \left(\bar{Q}_L \tilde{\mathbf{U}} \mathbf{Y}_Q \tau_3 Q_R - \text{h.c.} \right) + [Q_{L,R} \Rightarrow L_{L,R}],\tag{3.6}$$

and

$$\begin{aligned}\Delta \mathcal{L}_{\text{Bos}} &= -i \left(1 + \frac{h}{v} \right) \partial_\mu h \text{Tr} \left(\mathbf{T} \left(\partial^\mu \tilde{\mathbf{U}} \right) \tilde{\mathbf{U}}^\dagger \right) \left(\hat{a}_{2D} h + 4 \hat{a}_{13} \frac{\square h}{v^2} \right) \\ &\quad - i \text{Tr} \left(\mathbf{T} \left(\partial_\mu \partial^\mu \tilde{\mathbf{U}} \right) \tilde{\mathbf{U}}^\dagger \right) \left[\left(\hat{a}_{2D} - \frac{\hat{b}_{2D}}{4} \right) h^2 + 4 \left(\hat{a}_{13} - \frac{\hat{b}_{13}}{2} \right) \frac{h \square h}{v^2} \right. \\ &\quad \quad \left. - 2 \hat{b}_{13} \frac{\partial_\nu h \partial^\nu h}{v^2} + \frac{h^2}{2v} \left(\hat{a}_{2D} h + 4 \hat{a}_{13} \frac{\square h}{v^2} \right) \right] \\ &\quad - \left[g \text{Tr} (\mathbf{T} W^\mu) - g' B^\mu \right] \left[\left(\hat{a}_{2D} - \frac{\hat{b}_{2D}}{2} \right) h \partial_\mu h + 4 \left(\hat{a}_{13} - \frac{\hat{b}_{13}}{2} \right) \frac{h \partial^\mu \square h}{v^2} \right. \\ &\quad \quad \left. - 2 \hat{b}_{13} \left(\frac{\square h \partial_\mu h}{v^2} + 2 \frac{\partial_\nu h \partial_\mu \partial^\nu h}{v^2} \right) \right. \\ &\quad \quad \left. + \frac{h^2}{2v} \left(\hat{a}_{2D} \partial_\mu h + 4 \hat{a}_{13} \frac{\partial_\mu \square h}{v^2} \right) \right]\end{aligned}\tag{3.7}$$

where $\hat{b}_i \equiv c_i b_i$. The “tilde” over $\tilde{\mathbf{U}}$ will be dropped from now on.

Anomalous $q\bar{q}h$, $\ell\bar{\ell}h$ and Zhh vertices follow; the corresponding Feynman rules can be found in appendix B. It is worth to remark that if a generic $\mathcal{F}_i(h)$ function is considered also for the Yukawa terms instead of the SM-like dependence in eq. (2.2), further quartic $q\bar{q}h$ and $\ell\bar{\ell}h$ anomalous vertices will be revealed in addition to those shown in eq. (3.6); we postpone the analysis of these two-Higgs exotic interactions to a future publication.

In addition to the tree-level impact discussed, $\mathcal{S}_{2D}(h)$ and $\mathcal{S}_{13}(h)$ induce one-loop corrections to the Higgs gauge-boson couplings, see section 3.3, which in turn can be bounded from the strong experimental limits on fermionic EDMs, see eq. (3.42).

3.2 Triple gauge boson couplings

The operators in eq. (2.6) induce tree-level modifications of the self-couplings of the electroweak gauge bosons as well as of the Higgs-gauge boson vertices involving three or more particles: their impact on the Feynman rules of the theory are given in appendix B.

We first focus on the CP-violating triple gauge boson couplings $W^+W^-\gamma$ and W^+W^-Z , originated from the operators in eq. (2.6). Following ref. [97], the CP-odd sector of the Lagrangian that describes triple gauge boson vertices (TGVs) can be parametrised as:

$$\begin{aligned} \mathcal{L}_{\text{eff}, \mathcal{O}\mathcal{P}}^{WWV} = g_{WWV} \bigg(& g_4^V W_\mu^\dagger W_\nu (\partial^\mu V^\nu + \partial^\nu V^\mu) - i\tilde{\kappa}_V W_\mu^\dagger W_\nu \tilde{V}^{\mu\nu} - i\frac{\tilde{\lambda}_V}{M_W^2} W_{\sigma\mu}^\dagger W_\nu^\mu \tilde{V}^{\nu\sigma} \\ & + \tilde{g}_6^V (W_\nu^\dagger \partial_\mu W^\mu + W_\nu \partial_\mu W^{\dagger\mu}) V^\nu + \tilde{g}_7^V W_\mu^\dagger W^\mu \partial^\nu V_\nu \bigg), \end{aligned} \quad (3.8)$$

where $V \equiv \{\gamma, Z\}$ and $g_{WW\gamma} \equiv e = g \sin \theta_W$, $g_{WWZ} = g \cos \theta_W$. In this equation $W_{\mu\nu}^\pm$ and $V_{\mu\nu}$ stand exclusively for the kinetic part of the corresponding gauge field strengths, and the dual tensor $\tilde{V}_{\mu\nu}$ has been defined in section 2. In writing eq. (3.8) we have introduced the coefficients \tilde{g}_6^V and \tilde{g}_7^V associated to operators that contain the contraction $\mathcal{D}_\mu \mathbf{V}^\mu$; its $\partial_\mu \mathbf{V}^\mu$ part vanishes only for on-shell gauge bosons; in all generality $\mathcal{D}_\mu \mathbf{V}^\mu$ insertions could only be disregarded in the present context when fermion masses are neglected. In the SM all couplings in eq. (3.8) vanish.

Electromagnetic gauge invariance requires $g_4^\gamma = 0$, while the CP-odd bosonic operators in eq. (2.6) give the following contributions to the phenomenological coefficients in eq. (3.8):

$$\begin{aligned} \tilde{\kappa}_\gamma &= -\frac{4e^2}{s_\theta^2} (c_1 + 2c_8), & \tilde{\kappa}_Z &= \frac{4e^2}{c_\theta^2} \left(c_1 - 2\frac{c_\theta^2}{s_\theta^2} c_8 \right), \\ g_4^Z &= \frac{e^2}{2c_\theta^2 s_\theta^2} c_4, & \tilde{g}_6^Z &= \frac{e^2}{2c_\theta^2 s_\theta^2} (c_4 + c_{10}), \\ \tilde{g}_7^Z &= -\frac{e^2}{2c_\theta^2 s_\theta^2} (c_4 - 2c_{11}), & \tilde{g}_6^\gamma &= \tilde{g}_7^\gamma = \tilde{\lambda}_\gamma = \tilde{\lambda}_Z = 0. \end{aligned} \quad (3.9)$$

For completeness, note that there is an additional contribution to the ZZZ vertex of the form:

$$\mathcal{L}_{\text{eff}, \mathcal{O}\mathcal{P}}^{3Z} = \tilde{g}_{3Z} Z_\mu Z^\mu \partial_\nu Z^\nu, \quad (3.10)$$

with

$$\tilde{g}_{3Z} = \frac{e^3}{2c_\theta^3 s_\theta^3} (c_{10} + c_{11} + 2c_{16}), \quad (3.11)$$

which, alike to the phenomenological couplings \tilde{g}_6^V and \tilde{g}_7^V in eq. (3.8), vanishes for on-shell Z bosons and in general can be disregarded in the present context when the masses of fermions coupling to the Z are neglected.

It is interesting to compare the expected signals from the chiral Lagrangian presented here and the $d = 6$ linear realization. At the level of TGVs, there are six independent four-derivatives chiral CP-odd operators contributing to eqs. (3.9) and (3.10), while only two are present in the set of $d = 6$ linear ones. Furthermore the nature of the phenomenological

couplings involved is different, as some of the former correspond to $d = 8$ linear operators, while one of the latter set is a six derivatives. More explicitly, the two linear CP-odd operators at $d = 6$ are [8, 9]

$$\mathcal{O}_{\widetilde{W}B} = g g' \epsilon^{\mu\nu\rho\sigma} B_{\mu\nu} W_{\rho\sigma}^j \left(\Phi^\dagger \tau_j \Phi \right), \quad \mathcal{O}_{\widetilde{W}WW} = i \epsilon_{ijk} \widetilde{W}_\mu^{i\nu} W_\nu^{j\lambda} W_\lambda^{k\mu}, \quad (3.12)$$

where the first one is the sibling of $\mathcal{S}_1(h)$ (see appendix A) while $\mathcal{O}_{\widetilde{W}WW}$ does not have an equivalent operator in the chiral expansion up to four derivatives. Thus in this case the effective couplings in eq. (3.8) verify:

$$\begin{aligned} \tilde{\kappa}_\gamma^{(lin,d=6)} &= -\frac{c_\theta^2}{s_\theta^2} \tilde{\kappa}_Z^{(lin,d=6)}, & \tilde{\lambda}_\gamma^{(lin,d=6)} &= \tilde{\lambda}_Z^{(lin,d=6)}, \\ g_4^{Z,(lin,d=6)} &= \tilde{g}_6^{Z,(lin,d=6)} = \tilde{g}_7^{Z,(lin,d=6)} = \tilde{g}_6^{\gamma,(lin,d=6)} = \tilde{g}_7^{\gamma,(lin,d=6)} = 0. \end{aligned} \quad (3.13)$$

Hence, generically, if g_4^Z is found larger than $\tilde{\lambda}_\gamma$ or $\tilde{\lambda}_Z$, it would point out towards a chiral realization of the EWSB, while the contrary would signal towards the linear realization. Furthermore if non-zero $\tilde{\kappa}_\gamma$ and $\tilde{\kappa}_Z$ are observed, the relation in eq. (3.13) could be also tested.

The strongest constraints on CP violation in the $W^+W^-\gamma$ vertex arise from its contributions to fermionic EDMs that they can induce at one-loop, while constraints on CP-violating W^+W^-Z couplings can be obtained from the study of gauge-boson production at colliders. We further elaborate below in these two types of signals.

3.2.1 CP violation in $WW\gamma$: fermionic EDMs

Electric dipole moments for quarks and leptons are generically the best windows on BSM sources of CP-violation, due to the combination of the very stringent experimental bounds with the fact that they tend to be almost free from SM background contributions: fermionic EDMs are suppressed in the SM beyond two electroweak boson exchange, while in most BSM theories they are induced at one-loop level.

Although none of the operators in the chiral basis above — eq. (2.6) — induces tree-level contributions to EDMs, two of them, $\mathcal{S}_1(h)$ and $\mathcal{S}_8(h)$, contain gauge boson couplings involving the photon, of the form

$$+ \frac{i}{2} \epsilon_{\mu\nu\rho\sigma} W_\mu^+ W_\nu^- A^{\rho\sigma}, \quad (3.14)$$

where $A^{\rho\sigma}$ denotes the photon field strength, see eqs. (3.8) and (3.9) and appendix B. This coupling induces in turn a one-loop contribution to fermion EDMs, see figure 1.

The amplitude corresponding to this Feynman diagram can be parametrised as

$$\mathcal{A}_f \equiv -i d_f \bar{u}(p_2) \sigma_{\mu\nu} q^\nu \gamma^5 u(p_1), \quad (3.15)$$

where d_f denotes the fermionic EDM strength. The corresponding integral diverges logarithmically;⁵ assuming a physical cut-off Λ_s for the high energy BSM theory and following

⁵For a specific UV model which does not lead to logarithmic diverging EDM see [98].

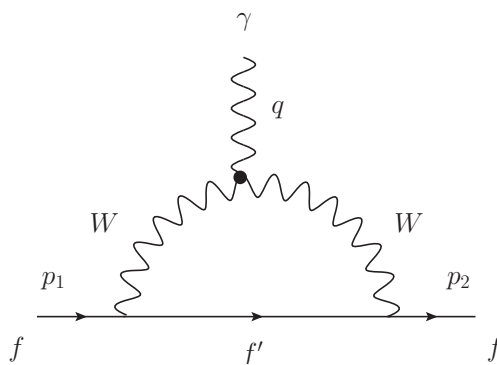


Figure 1. A CP-odd TGV coupling inducing a fermionic EDM interaction.

the generic computation in ref. [99], we obtain for the contribution from $\mathcal{S}_1(h)$ and $\mathcal{S}_8(h)$:

$$d_f = (c_1 + 2c_8) \frac{e^3 G_F T_{3L} \csc^2 \theta_W}{\sqrt{2} \pi^2} m_f \left[\log \left(\frac{\Lambda_s^2}{M_W^2} \right) + \mathcal{O}(1) \right], \quad (3.16)$$

where T_{3L} stands for the fermion weak isospin, θ_W denotes the Weinberg angle and G_F the Fermi coupling constant. The present experimental bound on the electron EDM [100],

$$\left| \frac{d_e}{e} \right| < 8.7 \times 10^{-29} \text{ cm}, \quad \text{at 90\% CL}, \quad (3.17)$$

implies then a limit

$$\left| (c_1 + 2c_8) \left[\log \left(\frac{\Lambda_s^2}{M_W^2} \right) + \mathcal{O}(1) \right] \right| < 5.2 \times 10^{-5}. \quad (3.18)$$

Using as values for the constituent quark masses $m_u = m_d = m_N/3$, the experimental limit on the neutron EDM [101],

$$\left| \frac{d_n}{e} \right| < 2.9 \times 10^{-26} \text{ cm}, \quad \text{at 90\% CL}, \quad (3.19)$$

allows to set an even stronger limit on the combination of $\mathcal{S}_1(h)$ and $\mathcal{S}_8(h)$ operator coefficients:

$$\left| (c_1 + 2c_8) \left[\log \left(\frac{\Lambda_s^2}{M_W^2} \right) + \mathcal{O}(1) \right] \right| < 2.8 \times 10^{-5}. \quad (3.20)$$

Weaker but more direct bounds on these operators can be imposed from the study of $W\gamma$ production at colliders. For example the recent study in ref. [102] concluded that the future 14 TeV LHC data with 10 fb^{-1} can place a 95% CL bound

$$|\tilde{\kappa}_\gamma| \leq 0.05 \quad \implies \quad |c_1 + 2c_8| \leq 0.03. \quad (3.21)$$

3.2.2 CP violation in WWZ : collider bounds and signatures

At present the strongest direct constraints on CP-violating effects in the WWZ vertex are imposed by the combination of results using the LEP collaboration studies on the observation of the angular distribution of W 's and their decay products in WW production at LEP II [103–105]. The combination yields the following 1σ (68% CL) constraints [106]

$$-0.47 \leq g_4^Z \leq -0.13, \quad -0.14 \leq \tilde{\kappa}_Z \leq -0.06, \quad -0.16 \leq \tilde{\lambda}_Z \leq -0.02, \quad (3.22)$$

which in terms of the coefficients of operators in eq. (2.6) implies

$$-1.8 \leq c_4 \leq -0.50, \quad -0.29 \leq \left(c_1 - 2 \frac{c_\theta^2}{s_\theta^2} c_8 \right) \leq -0.13. \quad (3.23)$$

Note that the bounds in eq. (3.22) are obtained assuming one effective coupling in eq. (3.8) being different from zero at a time, which is consistent with the predictions from the dynamical Higgs Lagrangian, eq. (3.9), since different operators lead to independent modifications of the effective couplings g_4^Z and $\tilde{\kappa}_Z$.

In what concerns Tevatron and LHC data, anomalous CP-odd TGV interactions have not been studied in detail yet. To fill this gap we present in what follows our analysis of the LHC potential to measure deviations or set exclusion bounds on CP-odd WWZ anomalous TGVs, extending our preliminary study [107]. At LEP the experimental analyses which lead to the bounds in eq. (3.22) were based on the study of the angular distributions of the final state particles in the event. In contrast, at the LHC, the higher collision energy — well above the WW and WZ thresholds — makes the use of kinematic variables related to the energy of the event more suitable for the measurement of TGV.

The study in ref. [107] concluded that the $pp \rightarrow W^\pm Z$ process has higher potential to observe g_4^Z than the $pp \rightarrow W^+W^-$ channel, while both channels have a similar power to study $\tilde{\kappa}_Z$ and $\tilde{\lambda}_Z$. Furthermore, it was also discussed the use of several kinematic distributions to characterize the presence of a non-vanishing CP-violating coupling and the use of some asymmetries to characterize its CP nature. So far the LHC has already collected almost 25 times more data than the luminosity considered in that preliminary study which we update here. In addition, in this update we take advantage of a more realistic background evaluation, by using the results of the experimental LHC analysis on other anomalous TGV interactions [108].⁶

In this section we study the process

$$pp \rightarrow \ell'^\pm \ell^+ \ell^- E_T^{\text{miss}}, \quad (3.24)$$

where $\ell^{(\prime)} = e$ or μ . The main background for the detection of anomalous TGV interactions is the irreducible SM production of $W^\pm Z$ pairs. In addition there are further reducible backgrounds like W or Z production with jets, ZZ production followed by the leptonic decay of the Z 's with one charged lepton escaping detection, and $t\bar{t}$ pair production.

⁶This strategy was also the starting point for the study of the CP conserving, but C and P violating coupling g_5^Z presented in ref. [54].

We simulate the signal and the SM irreducible background using an implementation of the anomalous vertices g_4^Z , $\tilde{\kappa}_Z$, and $\tilde{\lambda}_Z$ in FeynRules [109] interfaced with MadGraph 5 [110] for event generation. We account for the different detection efficiencies by rescaling our simulation of the SM production of $W^\pm Z$ pairs to the values quoted by ATLAS [108] for the study of $\Delta\kappa_Z$, g_1^Z and λ_Z . However, we have also cross-checked the results using a setup where the signal simulation is based on the same FeynRules [109] and MadGraph5 [110] implementation, interfaced then with PYTHIA [111] for parton shower and hadronization, and with PGS 4 [112] for detector simulation. Finally, the reducible backgrounds for the 7 TeV data analysis are obtained from the simulations presented in the ATLAS search [108], and they are properly rescaled for the 8 and 14 TeV runs.

In order to make our simulations more realistic, we closely follow the TGV analysis performed by ATLAS [108]. The kinematic study of the $W^\pm Z$ production starts with the usual detection and isolation cuts on the final state leptons. Muons and electrons are considered if their transverse momentum with respect to the collision axis z , $p_T \equiv \sqrt{p_x^2 + p_y^2}$, and their pseudorapidity $\eta \equiv \frac{1}{2} \ln \frac{|\vec{p}| + p_z}{|\vec{p}| - p_z}$, satisfy

$$\begin{aligned} p_T^\ell &> 15 \text{ GeV}, & |\eta^\mu| &< 2.5, \\ |\eta^e| &< 1.37 & \text{or} & 1.52 < |\eta^e| < 2.47. \end{aligned} \quad (3.25)$$

To guarantee the isolation of muons (electrons), we require that the scalar sum of the p_T of the particles within $\Delta R \equiv \sqrt{\Delta\eta^2 + \Delta\phi^2} = 0.3$ of the muon (electron), excluding the muon (electron) track, is smaller than 15% (13%) of the charged lepton p_T . In the cases when the final state contains both muons and electrons, a further isolation requirement has been imposed:

$$\Delta R_{e\mu} > 0.1. \quad (3.26)$$

It is also required that at least two leptons with the same flavour and opposite charge are present in the event and that their invariant mass is compatible with the Z mass, i.e.

$$M_{\ell+\ell-} \in [M_Z - 10, M_Z + 10] \text{ GeV}. \quad (3.27)$$

In what follows we refer to p^Z as the momentum of this $\ell^+\ell^-$ pair, $p^Z \equiv p^{\ell^+} + p^{\ell^-}$. We further impose that a third lepton is present which passes the above detection requirements and whose transverse momentum satisfies in addition

$$p_T^{\ell'} > 20 \text{ GeV}. \quad (3.28)$$

Moreover, with the purpose of suppressing most of the Z +jets and other diboson production backgrounds, we require

$$E_T^{\text{miss}} > 25 \text{ GeV} \quad \text{and} \quad M_T^W > 20 \text{ GeV}, \quad (3.29)$$

where E_T^{miss} is the missing transverse energy and the transverse mass is $M_T^W = \sqrt{2p_T^\ell E_T^{\text{miss}} (1 - \cos(\Delta\phi))}$, with $p_T^{\ell'}$ being the transverse momentum of the third lepton, and $\Delta\phi$ the azimuthal angle between the missing transverse momentum and the third

COM Energy	σ_{SM} (fb)	σ_{bck} (fb)	$\sigma_{\text{ano}}^{g_4^Z}$ (fb)	$\sigma_{\text{ano}}^{\tilde{\kappa}_Z}$	$\sigma_{\text{ano}}^{\tilde{\lambda}_Z}$
7 TeV	47.7	14.3	846	56.0	1914
8 TeV	55.3	16.8	1117	67.7	2556
14 TeV	97.0	29.0	3034	134	7471

Table 1. Values of the cross section predictions for the process $pp \rightarrow \ell'^{\pm} \ell^+ \ell^- E_T^{\text{miss}}$ after applying all the cuts described in the text. σ_{SM} is the SM contribution coming from EW $W^{\pm}Z$ production, σ_{ano}^i are the pure anomalous contributions and σ_{bck} corresponds to all the background sources except for the electroweak SM $W^{\pm}Z$ production.

lepton. Finally, it is required that at least one electron or one muon has a transverse momentum complying with

$$p_T^{e(\mu)} > 25 \text{ (20) GeV}. \quad (3.30)$$

Our Monte Carlo simulations have been tuned to the ATLAS ones [108], so as to incorporate more realistic detection efficiencies. Initially, a global k -factor is introduced to account for the higher order corrections to the process in eq. (3.24) by comparing our leading order predictions to the NLO ones used in the ATLAS search [108], leading to $k \sim 1.7$. Next, we compare our results after cuts with the ones quoted by ATLAS in table 1 of ref. [108]. We tune our simulation by applying a correction factor per flavour channel (eee , $ee\mu$, $e\mu\mu$ and $\mu\mu\mu$) that is almost equivalent to introducing a detection efficiency of $\epsilon^e = 0.8$ (0.95) for electrons (muons). These efficiencies have been employed in our simulations for signal and backgrounds.

After the selection procedure, in the presence of anomalous TGVs the cross section for the process $pp \rightarrow \ell'^{\pm} \ell^+ \ell^- E_T^{\text{miss}}$ can be qualitatively described by:

$$\sigma = \sigma_{\text{bck}} + \sigma_{SM} + \sum_{i,j \geq i} \sigma_{\text{ano}}^{ij} g_{\text{ano}}^i g_{\text{ano}}^j. \quad (3.31)$$

Here σ_{SM} corresponds to the irreducible SM $W^{\pm}Z$ background, while σ_{bck} stands for all background sources except for the SM EW $W^{\pm}Z$ production. Additionally σ_{ano}^{ij} are the pure anomalous contributions. Notice that because of the CP-violating nature of the anomalous couplings there is no interference between those and the SM contributing to the total cross section. Furthermore in the present study we assume only one coupling departing from its SM value at a time (i.e. always $i = j$) which, as mentioned above, is consistent with the expectations from the dynamical Higgs effective operators, eq. (3.9), since they lead to independent modifications of the two relevant effective couplings g_4^Z and $\tilde{\kappa}_Z$. We present in table 1 the values of σ_{SM} , σ_{bck} and σ_{ano} for center-of-mass energies of 7, 8 and 14 TeV.⁷

In order to quantify the reachable sensitivity on the determination of the different anomalous TGVs, advantage has been taken in this analysis of the fact that anomalous TGVs enhance the cross sections at high energies. Ref. [107] shows that the variables M_{WZ}^{rec}

⁷For completeness we make our study for the most general CP-violating WWZ vertex in eq. (3.8) and evaluate the sensitivity to $\tilde{\lambda}^Z$ as well, even though this coupling is generated at higher order in the chiral expansion as shown in eq. (3.9).

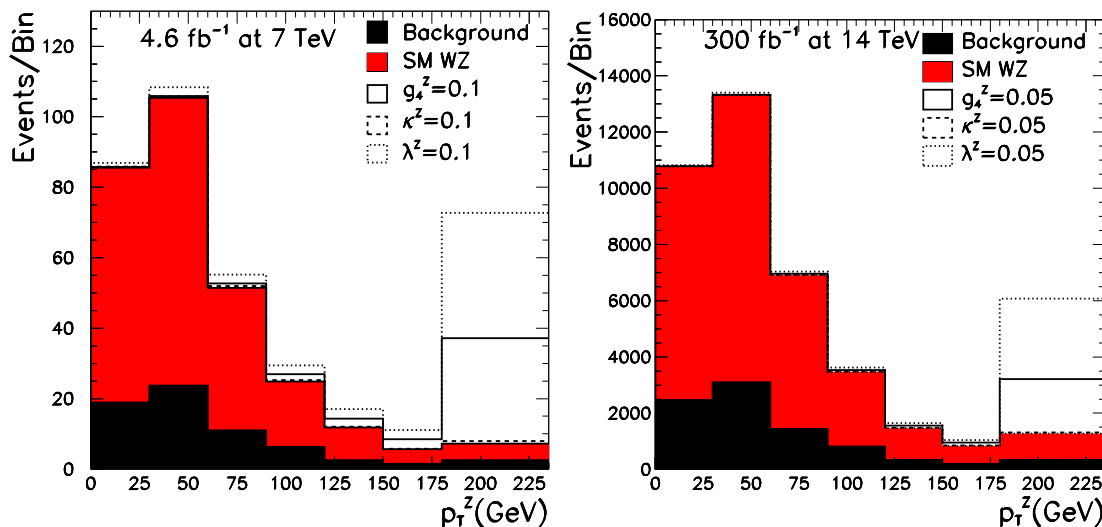


Figure 2. In the left (right) panel we show the distribution of events with respect to p_T^Z for the 7 (14) TeV run assuming $\mathcal{L} = 4.64$ (300) fb^{-1} of integrated luminosity. The black histogram contains all background sources, except for the SM $W^\pm Z$ production, the red histogram represents the sum of all the backgrounds and finally the solid (dashed) [dotted] distribution corresponds to the addition of the contribution of an anomalous TGV with a value $g_4^Z = 0.1$ ($\tilde{\kappa}_Z = 0.1$) [$\tilde{\lambda}_Z = 0.1$] for the 7 TeV run and $g_4^Z = 0.05$ ($\tilde{\kappa}_Z = 0.05$) [$\tilde{\lambda}_Z = 0.05$] for the 14 TeV run. The last bin contains all the events with $p_T^Z > 180$ GeV.

(the reconstructed WZ invariant mass), $p_T^{\ell \max}$ and p_T^Z are able to trace well this energy dependence, leading to similar sensitivities to the anomalous TGVs. Here, we chose p_T^Z because this variable is strongly correlated with the subprocess center-of-mass energy (\hat{s}), and, furthermore, it can be directly reconstructed with good precision from the measured lepton momenta. In the left (right) panel of figure 2 we show the number of expected events with respect to the transverse momentum of the Z candidate for the 7 (14) TeV run, assuming an integrated luminosity of $\mathcal{L} = 4.64$ (300) fb^{-1} . The figure captures the enhancement of events at the higher values of p_T^Z that the presence of anomalous TGV interactions causes. We can also observe how the effect of $\tilde{\kappa}_Z$ is weaker than the effect of introducing g_4^Z or $\tilde{\lambda}_Z$.

We have followed two procedures to estimate the LHC potential to probe anomalous CP-violating couplings. In a more conservative approach, we have performed a simple event counting analysis assuming that the number of observed events corresponds to the SM prediction, and we look for the values of the corresponding anomalous couplings which are inside the 68% and 95% CL allowed regions. In this case an additional cut $p_T^Z > 90$ GeV was applied in the analysis to enhance the sensitivity [107]. On a second analysis, a simple χ^2 has been built based on the contents of the different bins of the p_T^Z distribution, with the binning shown in figure 2. Once again, it is assumed that the observed p_T^Z spectrum corresponds to the SM expectations and we seek the values of the corresponding anomalous couplings that are inside the 68% and 95% allowed regions. In general the binned analysis yields 10% – 30% better sensitivity. The results of the binned analysis are presented in table 2.

	68% C.L. range		95% C.L. range	
	7+8 TeV	7+8+14 TeV	7+8 TeV	7+8+14 TeV
g_4^Z	(−0.019, 0.019)	(−0.007, 0.007)	(−0.027, 0.027)	(−0.010, 0.010)
$\tilde{\kappa}_Z$	(−0.12, 0.12)	(−0.047, 0.047)	(−0.17, 0.17)	(−0.067, 0.067)
$\tilde{\lambda}_Z$	(−0.012, 0.012)	(−0.004, 0.004)	(−0.018, 0.018)	(−0.006, 0.006)
c_4	(−0.074, 0.074)	(−0.027, 0.027)	(−0.10, 0.10)	(−0.039, 0.039)
$c_1 - 2\frac{c_\theta^2}{s_\theta^2}c_8$	(−0.25, 0.25)	(−0.099, 0.099)	(−0.36, 0.36)	(−0.14, 0.14)

Table 2. Expected sensitivity on g_4^Z , $\tilde{\kappa}_Z$ and $\tilde{\lambda}_Z$ at the LHC, and the corresponding precision reachable on the non-linear operator coefficients. We assume $\mathcal{L} = 4.64 \text{ fb}^{-1}$ for the 7 TeV run, $\mathcal{L} = 19.6 \text{ fb}^{-1}$ for the 8 TeV one and $\mathcal{L} = 300 \text{ fb}^{-1}$ for the future 14 TeV expectations.

From table 2 we read that the 7 and 8 TeV data sets could clearly increase the existing limits on g_4^Z , and consequently on c_4 , and the future 14 TeV run would rapidly approach the few per cent level. Conversely, as it was expected, the reachable sensitivity on $\tilde{\kappa}_Z$ is weaker. Nevertheless, the future 14 TeV run has the potential to improve the direct bounds that LEP was able to derive, and settle consequently the strongest direct available limits on the corresponding combination of c_1 and c_8 couplings. Notice that this combination is different from the c_1 and c_8 combination contributing to $\tilde{\kappa}_\gamma$, which is bounded from EDM measurements, see eqs. (3.9) and (3.21). Thus, both measurements are complementary.

Up to this point the analysis that we have performed has not benefitted from the CP-odd nature of the TGV interactions. Different studies [107, 113–115] have addressed the CP-odd nature of the anomalous TGVs by constructing some CP-odd or \hat{T} -odd observable. In particular, in ref. [114] it was shown that ideally in $pp \rightarrow W^\pm Z$ an asymmetric observable based on the sign of the cross-product $p_q \cdot (p_Z \times p_{\ell'})$ could be a direct probe of CP-violation, where here p_q is the four-momentum of the incoming quark. At the LHC, however, p_q cannot be fully determined and for this reason we build instead as a reconstructable correlated sign variable

$$\Xi_\pm \equiv \text{sign}(p^{\ell'})_z \text{sign}(p^{\ell'} \times p^Z)_z, \quad (3.32)$$

where z is the collision axis. We define the sign-weighted cross section as

$$\Delta\sigma \equiv \int d\sigma \Xi_\pm \equiv \sum_i g_{\text{ano}}^i \Delta\sigma_{\text{ano}}^i. \quad (3.33)$$

A CP-odd TGV gives a measurable contribution to this sign-weighted cross section which is linearly dependent on the coupling. On the contrary the SM background is symmetric with respect to Ξ_\pm and it gives a null contribution to the sign-weighted cross section in eq. (3.33). This behaviour is illustrated in figure 3 where we show the distribution of events at 14 TeV, assuming 300 fb^{-1} of integrated luminosity, with respect to the related variable

$$\cos\theta_\Xi \equiv \cos\theta^{\ell'} \cos\theta^{Z \times \ell'}, \quad (3.34)$$

where the angles are defined with respect to the z axis. In this form $\text{sign}(\cos\theta_\Xi) = \Xi_\pm$.

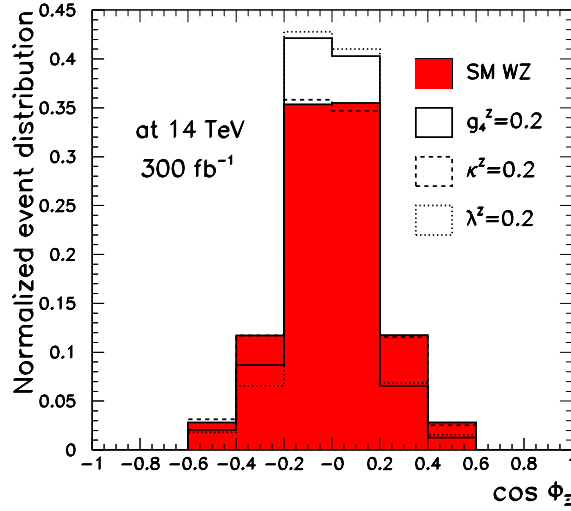


Figure 3. Distribution of $pp \rightarrow \ell'^{\pm} \ell^+ \ell^- E_T^{\text{miss}}$ contributions with respect to $\cos \theta_{\Xi}$, after the cuts described from eqs. (3.25)–(3.29) are applied, considering 300 fb^{-1} of integrated luminosity collected at 14 TeV. The sign-symmetric electroweak SM $W^{\pm}Z$ distribution is shown as the red histogram and the distribution for the SM plus the contribution of $g_4^Z = 0.2$ ($\tilde{\kappa}_Z = 0.2$) [$\tilde{\lambda}_Z = 0.2$] is shown as the solid (dashed) [dotted] line. All the distributions are normalized to one for an easier comparison.

The corresponding sign-weighted cross sections at 14 TeV are

$$\Delta\sigma_{\text{ano}}^{g_4^Z} = -59 \text{ fb}, \quad \Delta\sigma_{\text{ano}}^{\tilde{\kappa}_Z} = -9.7 \text{ fb}, \quad \Delta\sigma_{\text{ano}}^{\tilde{\lambda}_Z} = -137 \text{ fb}. \quad (3.35)$$

With a luminosity of 300 fb^{-1} this CP-violation induced asymmetry could be observed with 95% CL above the statistical fluctuations of the SM background for

$$|g_4^Z| \geq 0.02, \quad |\tilde{\kappa}_Z| \geq 0.13, \quad |\tilde{\lambda}_Z| \geq 0.01, \quad (3.36)$$

or what is equivalent for

$$|c_4| \geq 0.08, \quad \left| \left(c_1 - 2 \frac{c_{\theta}^2}{s_{\theta}^2} c_8 \right) \right| \geq 0.27. \quad (3.37)$$

3.3 CP violation in Higgs couplings to gauge-boson pairs

The effective operators described in eq. (2.6) also give rise to CP-odd interactions involving the Higgs particle and two gauge bosons, to which we refer as HVV couplings. The CP-odd interactions can be phenomenologically parametrized as

$$\begin{aligned} \mathcal{L}_{\text{eff}, \mathcal{CP}}^{\text{HVV}} = & \tilde{g}_{Hgg} h G_{\mu\nu}^a \tilde{G}^{a\mu\nu} + \tilde{g}_{H\gamma\gamma} h A_{\mu\nu} \tilde{A}^{\mu\nu} + \tilde{g}_{HZ\gamma} h A_{\mu\nu} \tilde{Z}^{\mu\nu} \\ & + \tilde{g}_{HZZ}^{(2)} h Z_{\mu\nu} \tilde{Z}^{\mu\nu} + \tilde{g}_{HWW}^{(2)} h W_{\mu\nu}^+ \tilde{W}^{-\mu\nu} \\ & + \left[\tilde{g}_{HWW}^{(1)} (W_{\mu\nu}^+ W^{-\mu} \partial^{\nu} h) + \text{h.c.} \right] + \left[\tilde{g}_{HWW}^{(5)} (\partial_{\mu} W^{+\mu} W_{\nu}^{-} \partial^{\nu} h) + \text{h.c.} \right], \end{aligned} \quad (3.38)$$

with tree level contributions

$$\begin{aligned}
 \tilde{g}_{Hgg} &= -\frac{g_S^2}{v} \hat{a}_{\tilde{G}}, & \tilde{g}_{H\gamma\gamma} &= \frac{4e^2}{v} \left(-\frac{1}{4} \hat{a}_{\tilde{B}} + \hat{a}_8 + \hat{a}_1 - \frac{1}{8} \hat{a}_{\tilde{W}} \right), \\
 \tilde{g}_{HZ\gamma} &= -\frac{8e^2 s_\theta}{vc_\theta} \left(-\frac{1}{4} \hat{a}_{\tilde{B}} - \frac{c_\theta^2}{2s_\theta^2} \left(-\frac{1}{4} \hat{a}_{\tilde{W}} + 2\hat{a}_8 \right) + \frac{1}{8s_\theta^2} (2\hat{a}_2 + \hat{a}_3 + 2\hat{a}_9) - \frac{c_{2\theta}}{2s_\theta^2} \hat{a}_1 \right), \\
 \tilde{g}_{HZZ}^{(2)} &= \frac{4e^2 s_\theta^2}{vc_\theta^2} \left(-\frac{1}{4} \hat{a}_{\tilde{B}} + \frac{c_\theta^4}{s_\theta^4} \hat{a}_8 - \frac{c_\theta^2}{s_\theta^2} \hat{a}_1 + \frac{1}{2s_\theta^2} \hat{a}_2 - \frac{c_\theta^4}{8s_\theta^4} \hat{a}_{\tilde{W}} - \frac{c_\theta^2}{2s_\theta^4} \hat{a}_9 - \frac{c_\theta^2}{4s_\theta^4} \hat{a}_3 \right), \\
 \tilde{g}_{HWW}^{(2)} &= -\frac{2e^2}{vs_\theta^2} \left(\frac{1}{2} \hat{a}_{\tilde{W}} + \hat{a}_3 \right), & \tilde{g}_{HWW}^{(1)} &= \frac{2e^2}{vs_\theta^2} i\hat{a}_7, & \tilde{g}_{HWW}^{(5)} &= -\frac{2e^2}{vs_\theta^2} i\hat{a}_{12},
 \end{aligned} \tag{3.39}$$

and where the \hat{a}_i coefficients have been defined in eq. (3.2). Additionally, the effective CP-odd Higgs-fermion couplings induced by the mixing effects described in section 3.1 generate one-loop induced HVV couplings such as

$$\tilde{g}_{Hgg} = \frac{\alpha_S}{8\pi v} \left(\hat{a}_{2D} - \frac{4p_h^2}{v^2} \hat{a}_{13} \right) F_{\text{odd}}^{\text{CP}}(x_f) = \frac{3}{8} \frac{\alpha_S}{\alpha_{\text{em}}} \tilde{g}_{H\gamma\gamma}, \tag{3.40}$$

where $F_{\text{odd}}^{\text{CP}}(x_f)$ is the form factor from the fermionic one-loop processes [116], that in the limit of high fermion masses ($x_f \equiv 4M_f^2/M_h^2 \gg 1$) is approximately $F_{\text{odd}}^{\text{CP}} = 1$, almost equal to the form factor for the CP-even Yukawa-fermion contribution to $hG_{\mu\nu}^a G^{a\mu\nu}$ and $hA_{\mu\nu} A^{\mu\nu}$ in the same limit, $F_{\text{even}}^{\text{CP}}(x_f)$. In addition to effects on the Higgs signals, these operators, together with those giving direct contributions to $\tilde{g}_{H\gamma\gamma}$ in eq. (3.39) give also a contribution to the fermion EDMs [117] of the form⁸

$$\begin{aligned}
 d_f &= \frac{e^3 m_f}{\pi^2 v^2} \left[-\frac{1}{4} \hat{a}_{\tilde{B}} + \hat{a}_8 + \hat{a}_1 - \frac{1}{8} \hat{a}_{\tilde{W}} + \frac{1}{48\pi^2} \hat{a}_{2D} \left(F_{\text{odd}}^{\text{CP}}(x_{\text{top}}) + \frac{2}{3} F_{\text{even}}^{\text{CP}}(x_{\text{top}}) \right) \right] \times \\
 &\quad \times \left[\log \frac{\Lambda_s^2}{m_H^2} + \mathcal{O}(1) \right], \tag{3.41}
 \end{aligned}$$

whose size can be constrained, for example, from the present bound on the electron EDM in eq. (3.19):

$$\begin{aligned}
 &\left| \left(-\frac{1}{4} \hat{a}_{\tilde{B}} + \hat{a}_8 + \hat{a}_1 - \frac{1}{8} \hat{a}_{\tilde{W}} + \frac{1}{48\pi^2} \hat{a}_{2D} \left(F_{\text{odd}}^{\text{CP}}(x_{\text{top}}) + \frac{2}{3} F_{\text{even}}^{\text{CP}}(x_{\text{top}}) \right) \right) \times \right. \\
 &\quad \left. \times \left[\log \left(\frac{\Lambda_s^2}{m_H^2} \right) + \mathcal{O}(1) \right] \right| < 5.6 \times 10^{-5}. \tag{3.42}
 \end{aligned}$$

While twelve chiral CP-odd operators affect HVV vertices, in the case of a linear realization of EWSB, at $d = 6$ only six operators contribute to eq. (3.38), which are the siblings of chiral operators $\mathcal{S}_1(h)$, $\mathcal{S}_2(h)$, $\mathcal{S}_3(h)$, $\mathcal{S}_G(h)$, $\mathcal{S}_B(h)$, $\mathcal{S}_W(h)$ listed in appendix A. Hence \tilde{g}_{Hgg} , $\tilde{g}_{H\gamma\gamma}$, $\tilde{g}_{HZ\gamma}$, $\tilde{g}_{HZZ}^{(2)}$, and $\tilde{g}_{HWW}^{(2)}$ can be generated at $d = 6$ with independent coefficients, while $\tilde{g}_{HWW}^{(1),(lin,d=6)} = \tilde{g}_{HWW}^{(5),(lin,d=6)} = 0$. Also one-loop HVV couplings will be induced by the $d = 6$ operator sibling of $\mathcal{S}_{2D}(h)$.

⁸In writing eq. (3.41) we have only considered the relevant loop of top quarks in the loop-induced part of the $h\gamma\gamma$ vertex (both CP-odd and CP-even) generated by $\mathcal{S}_{2D}(h)$ and we have neglected the corresponding $\mathcal{O}(m_f^2/m_H^2)$ contribution from $\mathcal{S}_{13}(h)$.

Generically because larger number of operators contribute to a given coupling in the chiral expansion, cancellations between their contributions can occur which are not possible in the case of the linear expansion at $d = 6$. However, we notice that for the HVV couplings in eq. (3.39) enough independent operators contribute in linear EWSB at $d = 6$ such that cancellations are also possible in this case.

Measuring the CP properties of the Higgs couplings is a subject with an extensive literature before and after the Higgs discovery. For the sake of concreteness we focus here on the experimental results on the most studied channel, $h \rightarrow ZZ \rightarrow \ell^+ \ell^- \ell'^+ \ell'^-$, for which combined results of the full 7+8 TeV LHC runs have been presented both by CMS [4, 118] and ATLAS [119, 120] collaborations.

Historically the key observables for measuring the CP properties of the Higgs in this channel were established in the seminal works in refs. [56–58], that were followed by an abundant literature on their applications to the LHC [59–65]. Most of these early phenomenological studies were based on the study of single variable observables. Most recently, an almost together with the first LHC collisions, two different new multivariable methods [66, 67] were proposed to use all the kinematic information of the event as input into the likelihood, to compare and exclude between different Higgs spin and parity hypothesis. These phenomenological studies set the roots of the first LHC experimental analyses of spin and CP properties of the Higgs in this channel [4, 118–120].

In particular the results of the experimental constraints from the CMS analysis [4, 118] can be translated into the language of the effective operators of a light dynamical Higgs in eq. (2.6). With this purpose we notice that in ref. [4] the $h \rightarrow ZZ$ vertex is described using the notation in [66]:

$$A(h \rightarrow ZZ) = v^{-1} \left(d_1 m_Z^2 \epsilon_1^* \epsilon_2^* + d_2 f_{\mu\nu}^{*(1)} f^{\mu\nu*(2)} + d_3 f_{\mu\nu}^{*(1)} \tilde{f}^{\mu\nu*(2)} \right), \quad (3.43)$$

where $f_{\mu\nu}^{(i)} = \epsilon_\mu^i q_\nu^i - \epsilon_\nu^i q_\mu^i$, $\tilde{f}_{\mu\nu}^{(i)} = \frac{1}{2} \epsilon_{\mu\nu\alpha\beta} f^{\alpha\beta(i)} = \epsilon_{\mu\nu\alpha\beta} \epsilon_i^\alpha q_i^\beta$, with $\epsilon^{1,2}$ being the polarization vectors of the Z bosons and $q_{1,2}$ the corresponding four-momenta. In the SM $d_1 = 2i$, while d_2 only receives marginally contributions from high order diagrams, that can be safely neglected leading to $d_2 = d_3 = 0$. The d_3 term is CP-odd and its interference with the CP-conserving terms d_1 or d_2 leads to the CP-violating signals that are analyzed.

The effective operators in eq. (2.6) give a non-vanishing contribution to d_3 which, from eqs. (3.38) and (3.39), reads

$$d_3 = -2iv\tilde{g}_{HZZ}^{(2)}, \quad (3.44)$$

while as long as no CP-conserving operators are considered $d_2 = 0$ and $d_1 = d_{1,SM}$.

In ref. [4] a measure of CP-violation in the $h \rightarrow ZZ^* \rightarrow 4\ell$ observables was defined as

$$f_{d_3} = \frac{|d_3|^2 \sigma_3}{|d_1|^2 \sigma_1 + |d_3|^2 \sigma_3}, \quad (3.45)$$

where σ_1 (σ_3) corresponds to the cross section for the process $h \rightarrow ZZ$ when $d_1 = 1$ ($d_3 = 1$) and $d_3 = 0$ ($d_1 = 1$). For $M_h = 125.6$ GeV, $\frac{\sigma_1}{\sigma_3} = 6.36$. In ref. [4] f_{d_3} was fitted as one of the parameters of the multivariable analysis, obtaining the measured value

$$f_{d_3} = 0.00_{-0.00}^{+0.17} \quad \Longrightarrow \quad \frac{|d_3|}{|d_1|} = 0.00_{-0.00}^{+1.14}, \quad (3.46)$$

pointing to the CP-even nature of the state. Furthermore, 95% CL exclusion bounds on f_{d_3} were derived,

$$f_{d_3} < 0.51 \quad \implies \quad \frac{|d_3|}{|d_1|} < 2.57. \quad (3.47)$$

We can directly translate the bounds in eq. (3.47) to 68(95)% CL constraints on the coefficients of the relevant CP-violating operators,

$$\left| -\frac{1}{4}\hat{a}_{\tilde{B}} + \frac{c_\theta^4}{s_\theta^4}\hat{a}_8 - \frac{c_\theta^2}{s_\theta^2}\hat{a}_1 + \frac{1}{2s_\theta^2}\hat{a}_2 - \frac{c_\theta^4}{8s_\theta^4}\hat{a}_{\tilde{W}} - \frac{c_\theta^2}{2s_\theta^4}\hat{a}_9 - \frac{c_\theta^2}{4s_\theta^4}\hat{a}_3 \right| \leq 10.3 \quad (23.3). \quad (3.48)$$

In ref. [121] the same analysis was applied to derive the future expectations when 300(3000) fb⁻¹ are collected at 14 TeV. The corresponding expected sensitivities at 95% CL are

$$f_{d_3} \leq 0.13 \text{ (0.04)} \quad \text{for} \quad 300 \text{ (3000)} \text{ fb}^{-1}. \quad (3.49)$$

They can be translated into the following sensitivity at 95% CL to the relevant combination of operators:

$$\left| -\frac{1}{4}\hat{a}_{\tilde{B}} + \frac{c_\theta^4}{s_\theta^4}\hat{a}_8 - \frac{c_\theta^2}{s_\theta^2}\hat{a}_1 + \frac{1}{2s_\theta^2}\hat{a}_2 - \frac{c_\theta^4}{8s_\theta^4}\hat{a}_{\tilde{W}} - \frac{c_\theta^2}{2s_\theta^4}\hat{a}_9 - \frac{c_\theta^2}{4s_\theta^4}\hat{a}_3 \right| \leq 8.8 \quad (4.6), \quad (3.50)$$

for 300 (3000) fb⁻¹.

Observables to study the CP properties of the Higgs couplings have also been proposed in the production channel $pp \rightarrow hjj$ followed by the Higgs decay into $\tau^+\tau^-$, W^+W^- , or $\gamma\gamma$ [68–78]. Depending on the kinematic cuts imposed, the study is most sensitive to CP-violating effects in the hWW (from $\mathcal{S}_{\tilde{W}}(h)$, $\mathcal{S}_3(h)$ and/or $\mathcal{S}_7(h)$) and hZZ (from $\mathcal{S}_{\tilde{B}}(h)$, $\mathcal{S}_{\tilde{W}}(h)$, $\mathcal{S}_1(h)$, $\mathcal{S}_2(h)$, $\mathcal{S}_3(h)$, $\mathcal{S}_8(h)$ and/or $\mathcal{S}_9(h)$) vertices contributing to Higgs production through vector boson fusion, or in the hgg vertex (from $\mathcal{S}_{\tilde{G}}(h)$, and from loop induced $\mathcal{S}_{2D}(h)$ and $\mathcal{S}_{13}(h)$) contributing to production by gluon fusion. The sensitivity to CP violating observables in associated production processes $pp \rightarrow hZ \rightarrow b\bar{b}\ell^+\ell^-$ and $pp \rightarrow hW \rightarrow \ell^+jjE_T^{\text{miss}}$ has also been studied in refs. [76, 79–83], and in pure gluon fusion production followed by Higgs decay into $\gamma\gamma$ or to $Z\gamma$ [84–87].

Finally, it is also possible to quantify the potential to observe or bound CP-odd interactions from global analyses of the Higgs signal strengths [35, 88, 89]. However in this case the analysis does not contain any genuinely CP-violating observable and consequently it is always sensitive to combinations of CP-even and CP-odd interactions.

4 Conclusions

Charge conjugation and parity are not exact symmetries of the Standard Model of particle physics, and furthermore electroweak interactions have proven that neither their product is a symmetry of nature. In addition, new sources of CP-violation are likely needed to explain the matter-antimatter asymmetry of the universe. More importantly, the extreme fine-tuning of the SM parameters implied by the strong CP problem suggests as well new sources of CP violation. On the other hand, the questions of whether the Higgs is elementary or composite, and of whether EWSB is realised linearly or non-linearly are still open.

We have focused here in the non-linear option for EWSB, approaching the issue through the model-independent tool of effective Lagrangians. We have established here for the first time the complete set of independent gauge and gauge-Higgs CP-odd effective operators for the generic case of a light dynamical Higgs, up to four derivatives in the chiral expansion, see the basis in eq. (2.6). The relation with the ensemble of $d = 6$ CP-odd linear operators has been clarified as well.

One interesting result is that an anomalous CP-odd coupling $\mathcal{S}_{2D}(h)$ is shown to be present already at the leading order of the chiral Lagrangian, that is, at the two-derivative level. It affects the renormalization of the SM parameters inducing a CP-odd component in fermion-Higgs and fermion- Z interactions. That coupling is instead not present at the leading order ($d = 4$) of the linear expansion, in other words in the SM Lagrangian, as its would-be linear sibling turns out to be a $d = 6$ operator. A similar contribution to two-point functions and with a similar physical impact stems as well from a four-derivative operator, $\mathcal{S}_{13}(h)$. Furthermore, focussing to triple gauge boson vertices, there are six independent four-derivatives chiral CP-odd operators contributing to these couplings, while only two are present in the set of $d = 6$ linear ones. Moreover, the nature of the phenomenological couplings involved is different, as some of the former correspond to $d = 8$ linear operators, while one of the latter set is a six derivatives. Considering instead the Higgs to two gauge boson vertices, there are in total twelve independent four-derivatives chiral CP-odd operators contributing to these interactions, while only seven are present for the $d = 6$ linear case.

We have established bounds on the CP-odd non-linear operator coefficients, mainly from anomalous triple vertices versus two types of experimental data: i) limits on fermionic EDMs which, not surprisingly given the very fine experimental precision, set some of the quantitatively tightest constraints; ii) present and future LHC data, in particular from the impact of TGV and Higgs-gauge boson triple couplings.

More precisely, among the TGV we have evaluated the one-loop contribution to fermionic EDMs from the anomalous CP-odd $WW\gamma$ vertex, and derived then the corresponding bounds on the relevant non-linear operator coefficients, see eqs. (3.18) and (3.20).

The bounds on the strength of anomalous CP-odd WWZ vertices have been explored here from both CP-blind and from CP-sensitive observables. The strongest limits are still coming from LEP analyses, and we have translated them into bounds for the non-linear operator coefficients, see eq. (3.23). Furthermore, the direct measurement of this vertex through CP-blind signals in gauge boson single or pair production at colliders has been addressed. In section 3.2.2 we have thus estimated the present and future potential of LHC to measure anomalous CP-odd TGVs performing a realistic collider analysis of WZ pair production. In doing so we have exploited that anomalous TGVs enhance the cross sections at high energies by quantifying the dependence of the expectations on kinematic variables which trace well this energy behaviour. The conclusion is that the LHC has the potential to improve the LEP bounds using the 7 and 8 TeV collected data sets, as shown in table 2, while the precision reachable in the future 14 TeV run will approach the per cent level on the anomalous coefficients.

Furthermore, on the realm of CP-odd observables, we have presented the LHC potential to decipher the CP nature of an hypothetical anomalous TGV observation by

defining CP-odd sensitive asymmetries. Through the asymmetry defined in eq. (3.33), it has been shown that the future LHC run will have the capability to establish the CP nature of the WWZ vertex for a large range of the parameter space that can be covered in that run, see eqs. (3.36) and (3.37).

For CP-odd observables sensitive to anomalous Higgs-gauge boson trilinear vertices, the focus has been set on the limits than can be obtained from the existing 7 and 8 TeV LHC experimental Higgs searches that benefit from genuinely CP-odd observables. We have translated the bounds from the CMS study of the Higgs boson properties on the leptonic $h \rightarrow ZZ$ channel to the relevant combination of non-linear operator coefficients, see eq. (3.48). The future sensitivity estimated by CMS in the same framework has also been translated into the future reachable sensitivity on the same combination of coefficients, eq. (3.50). Finally, we have also noticed that those combinations of non-linear operators contributing to the $h\gamma\gamma$ vertex can be constrained from the contribution of this trilinear coupling to fermionic EDMs, as illustrated in eq. (3.42).

The quest of new sources of CP-violation is well justified if not mandated by present observations and SM puzzles, while the elementary or composite nature of the Higgs and the maybe related nature –linear or non-linear– of the EWSB mechanism are other fundamental and urgent issues in particle physics. The model-independent theoretical analysis of CP violation performed in this paper for the case of a light dynamical Higgs, as well as the new limits established and the new phenomenological tools developed, should be useful in shedding light on these fundamental issues.

Acknowledgments

We thank O. Eboli for interesting discussions. We acknowledge partial support of the European Union network FP7 ITN INVISIBLES (Marie Curie Actions, PITN-GA-2011-289442), of CiCYT through the project FPA2009-09017, of the European Union FP7 ITN UNILHC (Marie Curie Actions, PITN-GA-2009-237920), of MICINN through the grant BES-2010-037869, of the Spanish MINECO Centro de Excelencia Severo Ochoa Programme under grant SEV-2012-0249, and of the Italian Ministero dell’Università e della Ricerca Scientifica through the COFIN program (PRIN 2008) and the contract MRTN-CT-2006-035505. M.C.G-G is supported by U.S.A.-NSF grant PHY-09-6739, and together with J.G-F by MICINN FPA2010-20807 and consolidator-ingenio 2010 program CSD-2008-0037. J.G-F is further supported by ME FPU grant AP2009-2546. The work of L.M. is supported by the Juan de la Cierva programme (JCI-2011-09244). The work of J.Y. is supported by the Spanish MINECO Centro de Excelencia Severo Ochoa Programme under grant SEV-2012-0249.

A Linear siblings of chiral operators

The interactions described by the chiral operators in eq. (2.6) can also be described in the context of a linearly realised EWSB, through linear operators built in terms of the SM Higgs doublet. In this appendix, the connection between the two expansions is discussed. As the number and nature of the leading order operators in the chiral and linear expansions

are not the same, an exact correspondence between the two kind of operators can be found only in the cases when $d = 6$ linear operators are involved, as only for them complete bases of independent terms have been defined. Otherwise, it will be indicated which chiral operators should be combined in order to generate the gauge interactions contained in specific $d > 6$ linear operators.

For chiral operators connected to $d = 6$ linear operators:

$$\begin{aligned}
 \mathcal{S}_{\tilde{B}}(h) &\rightarrow g'^2 \epsilon^{\mu\nu\rho\sigma} B_{\mu\nu} B_{\rho\sigma} \left(\Phi^\dagger \Phi \right) \\
 \mathcal{S}_{\tilde{W}}(h) &\rightarrow g^2 \epsilon^{\mu\nu\rho\sigma} \text{Tr} (W_{\mu\nu} W_{\rho\sigma}) \left(\Phi^\dagger \Phi \right) \\
 \mathcal{S}_{\tilde{G}}(h) &\rightarrow g_s^2 \epsilon^{\mu\nu\rho\sigma} G_{\mu\nu}^a G_{\rho\sigma}^a \left(\Phi^\dagger \Phi \right) \\
 \mathcal{S}_{2D}(h) &\rightarrow \left(\Phi^\dagger \overleftrightarrow{D}^\mu D_\mu \Phi \right) \left(\Phi^\dagger \Phi \right) \\
 \mathcal{S}_1(h) &\rightarrow g g' \epsilon^{\mu\nu\rho\sigma} B_{\mu\nu} W_{\rho\sigma}^j \left(\Phi^\dagger \tau_j \Phi \right) \\
 \mathcal{S}_2(h) &\rightarrow g' \epsilon^{\mu\nu\rho\sigma} B_{\mu\nu} \left[\left(\Phi^\dagger \overleftrightarrow{D}_\sigma D_\rho \Phi \right) + 2 (D_\rho \Phi)^\dagger D_\sigma \Phi \right] \\
 \mathcal{S}_3(h) &\rightarrow g \epsilon^{\mu\nu\rho\sigma} W_{\mu\nu}^i \left[\left(\Phi^\dagger \tau_i \overleftrightarrow{D}_\sigma D_\rho \Phi \right) + 2 (D_\rho \Phi)^\dagger \tau_i D_\sigma \Phi \right]
 \end{aligned} \tag{A.1}$$

For chiral operators connected to $d > 6$ linear operators:

$$\begin{aligned}
 \mathcal{S}_4(h) &\rightarrow g W_i^{\mu\nu} \left(\Phi^\dagger \tau^i \overleftrightarrow{D}_\mu \Phi \right) \left(\Phi^\dagger \overleftrightarrow{D}_\nu \Phi \right) & (d = 8) \\
 \mathcal{S}_5(h), \mathcal{S}_{10}(h) &\rightarrow (D^\mu \Phi)^\dagger (D^\nu \Phi) \left(\Phi^\dagger \overleftrightarrow{D}_\mu D_\nu \Phi \right) & (d = 8) \\
 \mathcal{S}_6(h), \mathcal{S}_{11}(h) &\rightarrow (D^\mu \Phi)^\dagger (D_\mu \Phi) \left(\Phi^\dagger \overleftrightarrow{D}^\nu D_\nu \Phi \right) & (d = 8) \\
 \mathcal{S}_7(h) &\rightarrow \epsilon_{ijk} W_{\mu\nu}^i \left(\Phi^\dagger \tau^j \overleftrightarrow{D}^\mu D^\nu \Phi \right) \left(\Phi^\dagger \tau^k \Phi \right) & (d = 8) \\
 \mathcal{S}_8(h) &\rightarrow g^2 \epsilon^{\mu\nu\rho\sigma} W_{\mu\nu}^i W_{\rho\sigma}^j \left(\Phi^\dagger \tau_i \Phi \right) \left(\Phi^\dagger \tau_j \Phi \right) & (d = 8) \\
 \mathcal{S}_9(h) &\rightarrow g \epsilon^{\mu\nu\rho\sigma} W_{\mu\nu}^i \left(\Phi^\dagger \tau^i \Phi \right) \left(\Phi^\dagger \overleftrightarrow{D}_\rho D_\sigma \Phi \right) & (d = 8) \\
 \mathcal{S}_{12}(h), \mathcal{S}_{13}(h), \mathcal{S}_{14}(h) &\rightarrow \left(\Phi^\dagger \overleftrightarrow{D}^\mu D_\mu \Phi \right) D^\nu D_\nu \left(\Phi^\dagger \Phi \right) & (d = 8) \\
 \mathcal{S}_{15}(h), \mathcal{S}_{16}(h) &\rightarrow \left(\Phi^\dagger \overleftrightarrow{D}^\mu \Phi \right) \left(\Phi^\dagger \overleftrightarrow{D}_\mu \Phi \right) \left(\Phi^\dagger \overleftrightarrow{D}^\nu D_\nu \Phi \right) & (d = 10)
 \end{aligned} \tag{A.2}$$

where in the brackets the dimension of the specific linear operator is explicitly reported.

B Feynman rules

This appendix provides a complete list of all Feynman rules resulting from the CP-odd operators in the Lagrangian $\Delta\mathcal{L}_{\text{CP}}$ in eqs. (2.5) and (2.6). Greek indexes denote the flavour of the fermionic legs and are assumed to be summed over when repeated; whenever they do not appear, it should be understood that the vertex is flavour diagonal. Moreover,

\mathbf{y}_f ($f = U, D, E$) denotes the eigenvalue of the corresponding Yukawa coupling matrix defined in eq. (2.4). Chirality operators $P_{L,R}$ are defined as

$$P_L = \frac{1}{2} (1 - \gamma^5) , \quad P_R = \frac{1}{2} (1 + \gamma^5) . \quad (\text{B.1})$$

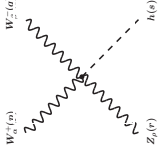
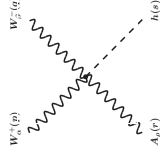
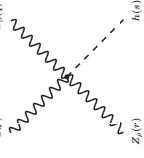
Flow in momentum convention is assumed in all diagrams. Only diagrams with up to four legs are shown and the expansion for $\mathcal{F}_i(h)$ in eq. (2.7) has been adopted, together with the definitions of the \hat{a}_i coefficients in eq. (3.2) and $\hat{b}_i = c_i b_i$. Vertices cubic in h have been omitted below, but for eq. (FR.26) which results from the product of two $F_i(h)$ functions, see Footnote 5. Finally, the SM and BSM Lorentz structures are reported in two distinct columns, on the left and on the right, respectively. Notice that all the pure gauge and gauge- h interactions have no SM contribution. All quantities entering in the Feynman rules below have resulted after the Z -renormalization scheme has been implemented.

	SM	Non-SM
(FR.1)	$A_\mu(p) \text{ } \text{~~~~~} \text{ } A_\nu(p)$	$\frac{-i}{p^2} \left[g^{\mu\nu} - (1 - \eta) \frac{p^\mu p^\nu}{p^2} \right]$ (η is the gauge fixing parameter)
(FR.2)	$Z_\mu(p) \text{ } \text{~~~~~} \text{ } Z_\nu(p)$	$\frac{-i}{p^2 - m_Z^2} \left[g^{\mu\nu} - (1 - \eta) \frac{p^\mu p^\nu}{p^2 - \eta m_Z^2} \right]$
(FR.3)	$W_\mu^+(p) \text{ } \text{~~~~~} \text{ } W_\nu^-(p)$	$\frac{-i}{p^2 - m_W^2} \left[g^{\mu\nu} - (1 - \eta) \frac{p^\mu p^\nu}{p^2 - \eta m_W^2} \right]$
(FR.4)	$G_\mu^a(p) \text{ } \text{~~~~~} \text{ } G_\nu^b(p)$	$\frac{-i g^{\mu\nu}}{p^2} \left[g^{\mu\nu} - (1 - \eta) \frac{p^\mu p^\nu}{p^2} \right]$
(FR.5)	$h(p) \text{ } \text{-----} \text{ } h(p)$	$\frac{-i}{p^2 - m_h^2}$
(FR.6)	$f(p) \text{ } \text{-----} \text{ } f(p)$	$\frac{i(\not{p} + m_f)}{p^2 - m_f^2}; \quad m_f = -\frac{v \mathbf{y}_f}{\sqrt{2}},$ $f = U, D, E$

	SM	Non-SM
(FR.7)		$+8ie^3 [c_8 \cot \theta_W \csc^2 \theta_W - c_1 \csc(2\theta_W)] (p_\sigma + q_\sigma) \epsilon^{\alpha\beta\rho\sigma}$ $e^3 \csc^2 \theta_W \csc(2\theta_W) \{ -2c_{11} g^{\alpha\beta} (p^\rho + q^\rho) + c_{10} (g^{\beta\rho} p^\alpha + g^{\alpha\rho} q^\beta) \\ + c_4 [g^{\beta\rho} (p^\alpha + r^\alpha) + g^{\alpha\rho} (q^\beta + r^\beta) + g^{\alpha\beta} (p^\rho + q^\rho)] \} +$
(FR.8)		$4ie^3 \csc^2 \theta_W (2c_8 + c_1) (p_\sigma + q_\sigma) \epsilon^{\alpha\beta\rho\sigma}$
(FR.9)		$8e^3 (2c_{16} + c_{10} + c_{11}) \csc^3(2\theta_W) [g^{\beta\rho} p^\alpha + g^{\alpha\rho} q^\beta - g^{\alpha\beta} (p^\rho + q^\rho)]$
(FR.10)		$(c_4 + c_{10}) e^4 \csc^2 \theta_W \csc(2\theta_W) (g^{\alpha\sigma} g^{\beta\rho} - g^{\alpha\rho} g^{\beta\sigma})$

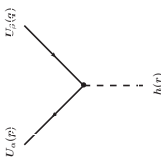
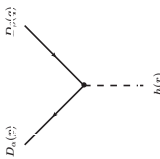
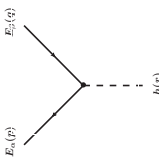
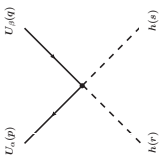
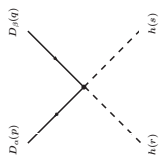
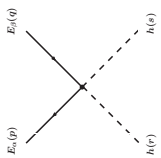
	SM	Non-SM
(FR.11)		$\frac{8i}{v} e^2 [2(-\frac{1}{4} \hat{a}_{\tilde{B}} + \hat{a}_8 + \hat{a}_1) - \frac{1}{4} \hat{a}_{\tilde{W}}] p_\mu q_\nu \epsilon^{\alpha\beta\mu\nu}$
(FR.12)		$-\frac{4i}{v} e^2 [4(-\frac{1}{4} \hat{a}_{\tilde{B}} + \hat{a}_8 + \hat{a}_1) - 2(-\frac{1}{2} \hat{a}_{\tilde{B}} + \hat{a}_2) \sec^2 \theta_W \\ + \csc^2 \theta_W (\frac{1}{2} \hat{a}_{\tilde{W}} - 4 \hat{a}_8 + 2 \hat{a}_9 + \hat{a}_3) - \frac{1}{2} \hat{a}_{\tilde{W}}] p_\mu q_\nu \epsilon^{\alpha\beta\mu\nu}$
(FR.13)		$-\frac{4i}{v} e^2 [-\hat{a}_{\tilde{B}} \tan \theta_W - 2 \cot \theta_W (-\frac{1}{4} \hat{a}_{\tilde{W}} + 2 \hat{a}_8) \\ + (2 \hat{a}_9 + 2 \hat{a}_2 + \hat{a}_3) \csc(2\theta_W) - 4 \hat{a}_1 \cot(2\theta_W)] p_\mu q_\nu \epsilon^{\alpha\beta\mu\nu}$

	SM	Non-SM
(FR.14)		$-\frac{4i}{v} g_s^2 \delta^{ab} \hat{a}_{\mathfrak{G}} p_\mu q_\nu \epsilon^{\alpha\beta\mu\nu}$
(FR.15)		$\frac{2}{v} e^2 \csc^2 \theta_W [\hat{a}_7 g^{\alpha\beta} (p \cdot p - q \cdot q) - (\hat{a}_7 - \hat{a}_{12}) (p^\alpha p^\beta - q^\alpha q^\beta)]$ $-\frac{4i}{v} e^2 \csc^2 \theta_W (\hat{a}_3 + \frac{1}{2} \hat{a}_{\bar{W}}) p_\mu q_\nu \epsilon^{\alpha\beta\mu\nu}$
(FR.16)		$\frac{2}{v^2} e \csc(2\theta_W) \left\{ 8 \hat{a}_{14} a'_{14} (r \cdot s) p^\alpha + v^2 \left[\left(\hat{a}_{2D} - \frac{\hat{b}_{2D}}{2} \right) p^\alpha \right. \right.$ $\left. \left. + \frac{4}{v^2} \hat{a}_{13} (r^2 r^\alpha + s^2 s^\alpha) + \frac{2}{v^2} \hat{b}_{13} p^2 p^\alpha \right] \right\}$

SM	Non-SM
 <p style="text-align: center;">(FR.17)</p>	$ \begin{aligned} & \frac{1}{v} e^3 \csc^3 \theta_W \sec \theta_W \left\{ \hat{a}_{10} g^{\beta\rho} p^\alpha + \hat{a}_7 [g^{\beta\rho} (p^\alpha + q^\alpha + r^\alpha) + g^{\alpha\rho} (p^\beta + q^\beta + r^\beta)] + \hat{a}_{12} [g^{\beta\rho} (p^\alpha + q^\alpha + r^\alpha) + \right. \\ & + g^{\alpha\rho} (p^\beta + q^\beta + r^\beta)] + \hat{a}_{10} g^{\alpha\rho} q^\beta - 2 \hat{a}_6 g^{\alpha\beta} (p^\rho + q^\rho + r^\rho) - 2 \hat{a}_7 g^{\alpha\beta} (p^\rho + q^\rho + r^\rho) + 2 \hat{a}_{11} g^{\alpha\beta} r^\rho + \\ & - \hat{a}_5 [g^{\beta\rho} (p^\alpha + q^\alpha + r^\alpha) + g^{\alpha\rho} (p^\beta + q^\beta + r^\beta)] - \hat{a}_4 [g^{\beta\rho} q^\alpha + g^{\alpha\rho} p^\beta - g^{\alpha\beta} (p^\rho + q^\rho)] + \\ & + \cos(2\theta_W) \left[(\hat{a}_7 - \hat{a}_{12}) (g^{\beta\rho} (p^\alpha + q^\alpha + r^\alpha) + g^{\alpha\rho} (p^\beta + q^\beta + r^\beta)) - 2 \hat{a}_7 g^{\alpha\beta} (p^\rho + q^\rho + r^\rho) \right] \Big\} + \\ & + \frac{2i}{v} e^3 \csc^3 \theta_W \sec \theta_W \left\{ 4 \cos^2 \theta_W \left[\frac{1}{4} \hat{a}_{\tilde{W}} (p_\sigma + q_\sigma + r_\sigma) - 2 \hat{a}_8 r_\sigma \right] + 2 \hat{a}_9 (p_\sigma + q_\sigma + r_\sigma) + \right. \\ & \quad \left. + \hat{a}_3 [\cos(2\theta_W) + 2] (p_\sigma + q_\sigma + r_\sigma) + 4 \hat{a}_1 r_\sigma \sin^2 \theta_W \right\} \epsilon^{\alpha\beta\rho\sigma} \end{aligned} $
 <p style="text-align: center;">(FR.18)</p>	$ \begin{aligned} & \frac{2}{v} e^3 \csc^2 \theta_W \left\{ (\hat{a}_7 - \hat{a}_{12}) [g^{\beta\rho} (p^\alpha + q^\alpha + r^\alpha) + g^{\alpha\rho} (p^\beta + q^\beta + r^\beta)] - 2 \hat{a}_7 g^{\alpha\beta} (p^\rho + q^\rho + r^\rho) \right\} + \\ & - \frac{4i}{v} e^3 \csc^2 \theta_W \left[-\frac{1}{2} \hat{a}_{\tilde{W}} (p_\sigma + q_\sigma + r_\sigma) - \hat{a}_3 (p_\sigma + q_\sigma + r_\sigma) + 2 (2 \hat{a}_8 + \hat{a}_1) r_\sigma \right] \epsilon^{\alpha\beta\rho\sigma} \end{aligned} $
 <p style="text-align: center;">(FR.19)</p>	$ \begin{aligned} & \frac{1}{v} 16 e^3 \csc^3(2\theta_W) \left\{ (2 \hat{a}_{16} + \hat{a}_{10} + \hat{a}_{11}) (g^{\beta\rho} p^\alpha + g^{\alpha\rho} q^\beta + g^{\alpha\beta} r^\rho) + \right. \\ & \quad \left. - (2 \hat{a}_{15} + \hat{a}_5 + \hat{a}_6) [g^{\beta\rho} (p^\alpha + q^\alpha + r^\alpha) + g^{\alpha\rho} (p^\beta + q^\beta + r^\beta)] + g^{\alpha\beta} (p^\rho + q^\rho + r^\rho) \right\} \end{aligned} $

	SM	Non-SM
(FR.20)		$\frac{4}{v} f^{abc} g_s^3 \hat{a}_{\tilde{\Phi}} (p_\mu + q_\mu + r_\mu) \epsilon^{\alpha\beta\mu\rho}$
(FR.21)		$\frac{8i}{v^2} e^2 \left[2 \left(-\frac{1}{4} \hat{b}_{\tilde{B}} + \hat{b}_8 + \hat{b}_1 \right) - \frac{1}{4} \hat{b}_{\tilde{W}} \right] p_\mu q_\nu \epsilon^{\alpha\beta\mu\nu}$
(FR.22)		$-\frac{4i}{v^2} e^2 \left[4 \left(-\frac{1}{4} \hat{b}_{\tilde{B}} + \hat{b}_8 + \hat{b}_1 \right) - 2 \left(-\frac{1}{2} \hat{b}_{\tilde{B}} + \hat{b}_2 \right) \sec^2 \theta_W \right. \\ \left. + \csc^2 \theta_W \left(\frac{1}{2} \hat{b}_{\tilde{W}} - 4 \hat{b}_8 + 2 \hat{b}_9 + \hat{b}_3 \right) - \frac{1}{2} \hat{b}_{\tilde{W}} \right] p_\mu q_\nu \epsilon^{\alpha\beta\mu\nu}$
(FR.23)		$-\frac{4i}{v^2} e^2 \left[-\hat{b}_{\tilde{B}} \tan \theta_W - 2 \cot \theta_W \left(-\frac{1}{4} \hat{b}_{\tilde{W}} + 2 \hat{b}_8 \right) \right. \\ \left. + \left(2 \hat{b}_9 + 2 \hat{b}_2 + \hat{b}_3 \right) \csc(2\theta_W) - 4 \hat{b}_1 \cot(2\theta_W) \right] p_\mu q_\nu \epsilon^{\alpha\beta\mu\nu}$

	SM	Non-SM
(FR.24)		$\frac{2}{v^2} e^2 \csc^2 \theta_W \left\{ \hat{b}_7 \left[g^{\alpha\beta} (q \cdot r - p \cdot r) + p^\beta r^\alpha - q^\alpha r^\beta \right] \right. \\ \left. + \hat{b}_{12} (q^\beta r^\alpha - p^\alpha r^\beta) \right\} - \frac{2i}{v^2} e^2 \left(\hat{b}_3 + \hat{b}_{\tilde{W}} \right) \csc^2 \theta_W p_\mu q_\nu \epsilon^{\alpha\beta\mu\nu}$
(FR.25)		$-\frac{4i}{v^2} g_s^2 \delta^{ab} \hat{b}_{\tilde{\Phi}} p_\mu q_\nu \epsilon^{\alpha\beta\mu\nu}$
(FR.26)		$\frac{2}{v^3} e \csc(2\theta_W) \left\{ 8 p^\alpha (r \cdot q + q \cdot s + r \cdot s) \left(\hat{a}_{14} b'_{14} + \hat{b}_{14} a'_{14} \right) \right. \\ \left. + v^2 \left[\hat{a}_{2D} p^\alpha + \frac{4}{v^2} \hat{a}_{13} (q^2 q^\alpha + r^2 r^\alpha + s^2 s^\alpha) \right] \right\}$

SM		Non-SM	
<div>  </div>	(FR.27)	$-\frac{i}{\sqrt{2}} \left[P_L \left(Y_U^\dagger \right)_{\alpha\beta} + P_R \left(Y_U \right)_{\alpha\beta} \right] + \frac{1}{\sqrt{2} v^2} \left(\hat{a}_{2D} v^2 - 4 \hat{a}_{13} r^2 \right) \left[P_L \left(Y_U^\dagger \right)_{\alpha\beta} - P_R \left(Y_U \right)_{\alpha\beta} \right]$	
<div>  </div>	(FR.28)	$-\frac{i}{\sqrt{2}} \left[P_L \left(Y_D^\dagger \right)_{\alpha\beta} + P_R \left(Y_D \right)_{\alpha\beta} \right] - \frac{1}{\sqrt{2} v^2} \left(\hat{a}_{2D} v^2 - 4 \hat{a}_{13} r^2 \right) \left[P_L \left(Y_D^\dagger \right)_{\alpha\beta} - P_R \left(Y_D \right)_{\alpha\beta} \right]$	
<div>  </div>	(FR.29)	$-\frac{i}{\sqrt{2}} \left[P_L \left(Y_E^\dagger \right)_{\alpha\beta} + P_R \left(Y_E \right)_{\alpha\beta} \right] - \frac{1}{\sqrt{2} v^2} \left(\hat{a}_{2D} v^2 - 4 \hat{a}_{13} r^2 \right) \left[P_L \left(Y_E^\dagger \right)_{\alpha\beta} - P_R \left(Y_E \right)_{\alpha\beta} \right]$	
SM		Non-SM	
<div>  </div>	(FR.30)	$+\frac{\sqrt{2}}{v^3} \left[\hat{a}_{2D} v^2 - 2 \hat{a}_{13} \left(r^2 + s^2 \right) \right] \left[P_L \left(Y_U^\dagger \right)_{\alpha\beta} - P_R \left(Y_U \right)_{\alpha\beta} \right]$	
<div>  </div>	(FR.31)	$-\frac{\sqrt{2}}{v^3} \left[\hat{a}_{2D} v^2 - 2 \hat{a}_{13} \left(r^2 + s^2 \right) \right] \left[P_L \left(Y_D^\dagger \right)_{\alpha\beta} - P_R \left(Y_D \right)_{\alpha\beta} \right]$	
<div>  </div>	(FR.32)	$-\frac{\sqrt{2}}{v^3} \left[\hat{a}_{2D} v^2 - 2 \hat{a}_{13} \left(r^2 + s^2 \right) \right] \left[P_L \left(Y_E^\dagger \right)_{\alpha\beta} - P_R \left(Y_E \right)_{\alpha\beta} \right]$	

Open Access. This article is distributed under the terms of the Creative Commons Attribution License ([CC-BY 4.0](https://creativecommons.org/licenses/by/4.0/)), which permits any use, distribution and reproduction in any medium, provided the original author(s) and source are credited.

References

- [1] CMS collaboration, *Combination of Standard Model Higgs boson searches and measurements of the properties of the new boson with a mass near 125 GeV*, [CMS-PAS-HIG-13-005](#), CERN, Geneva Switzerland (2013).
- [2] ATLAS collaboration, *Updated coupling measurements of the Higgs boson with the ATLAS detector using up to 25 fb⁻¹ of proton-proton collision data*, [ATLAS-CONF-2014-009](#), CERN, Geneva Switzerland (2014).
- [3] ATLAS collaboration, *Measurements of Higgs boson production and couplings in diboson final states with the ATLAS detector at the LHC*, *Phys. Lett. B* **726** (2013) 88 [[arXiv:1307.1427](#)] [[INSPIRE](#)].
- [4] CMS collaboration, *Measurement of the properties of a Higgs boson in the four-lepton final state*, *Phys. Rev. D* **89** (2014) 092007 [[arXiv:1312.5353](#)] [[INSPIRE](#)].
- [5] F. Englert and R. Brout, *Broken symmetry and the mass of gauge vector mesons*, *Phys. Rev. Lett.* **13** (1964) 321 [[INSPIRE](#)].
- [6] P.W. Higgs, *Broken symmetries, massless particles and gauge fields*, *Phys. Lett.* **12** (1964) 132 [[INSPIRE](#)].
- [7] P.W. Higgs, *Broken symmetries and the masses of gauge bosons*, *Phys. Rev. Lett.* **13** (1964) 508 [[INSPIRE](#)].
- [8] W. Buchmüller and D. Wyler, *Effective Lagrangian analysis of new interactions and flavor conservation*, *Nucl. Phys. B* **268** (1986) 621 [[INSPIRE](#)].
- [9] B. Grzadkowski, M. Iskrzynski, M. Misiak and J. Rosiek, *Dimension-six terms in the Standard Model Lagrangian*, *JHEP* **10** (2010) 085 [[arXiv:1008.4884](#)] [[INSPIRE](#)].
- [10] K. Hagiwara, S. Ishihara, R. Szalapski and D. Zeppenfeld, *Low-energy effects of new interactions in the electroweak boson sector*, *Phys. Rev. D* **48** (1993) 2182 [[INSPIRE](#)].
- [11] K. Hagiwara, T. Hatsukano, S. Ishihara and R. Szalapski, *Probing nonstandard bosonic interactions via W boson pair production at lepton colliders*, *Nucl. Phys. B* **496** (1997) 66 [[hep-ph/9612268](#)] [[INSPIRE](#)].
- [12] K. Hagiwara, R. Szalapski and D. Zeppenfeld, *Anomalous Higgs boson production and decay*, *Phys. Lett. B* **318** (1993) 155 [[hep-ph/9308347](#)] [[INSPIRE](#)].
- [13] M.C. Gonzalez-Garcia, *Anomalous Higgs couplings*, *Int. J. Mod. Phys. A* **14** (1999) 3121 [[hep-ph/9902321](#)] [[INSPIRE](#)].
- [14] I. Low, J. Lykken and G. Shaughnessy, *Have we observed the Higgs (imposter)?*, *Phys. Rev. D* **86** (2012) 093012 [[arXiv:1207.1093](#)] [[INSPIRE](#)].
- [15] T. Corbett, O.J.P. Eboli, J. Gonzalez-Fraile and M.C. Gonzalez-Garcia, *Constraining anomalous Higgs interactions*, *Phys. Rev. D* **86** (2012) 075013 [[arXiv:1207.1344](#)] [[INSPIRE](#)].
- [16] J. Ellis and T. You, *Global analysis of the Higgs candidate with mass ~ 125 GeV*, *JHEP* **09** (2012) 123 [[arXiv:1207.1693](#)] [[INSPIRE](#)].

- [17] P.P. Giardino, K. Kannike, M. Raidal and A. Strumia, *Is the resonance at 125 GeV the Higgs boson?*, *Phys. Lett. B* **718** (2012) 469 [[arXiv:1207.1347](#)] [[INSPIRE](#)].
- [18] M. Montull and F. Riva, *Higgs discovery: the beginning or the end of natural EWSB?*, *JHEP* **11** (2012) 018 [[arXiv:1207.1716](#)] [[INSPIRE](#)].
- [19] J.R. Espinosa, C. Grojean, M. Muhlleitner and M. Trott, *First glimpses at Higgs' face*, *JHEP* **12** (2012) 045 [[arXiv:1207.1717](#)] [[INSPIRE](#)].
- [20] D. Carmi, A. Falkowski, E. Kuflik, T. Volansky and J. Zupan, *Higgs after the discovery: a status report*, *JHEP* **10** (2012) 196 [[arXiv:1207.1718](#)] [[INSPIRE](#)].
- [21] S. Banerjee, S. Mukhopadhyay and B. Mukhopadhyaya, *New Higgs interactions and recent data from the LHC and the Tevatron*, *JHEP* **10** (2012) 062 [[arXiv:1207.3588](#)] [[INSPIRE](#)].
- [22] F. Bonnet, T. Ota, M. Rauch and W. Winter, *Interpretation of precision tests in the Higgs sector in terms of physics beyond the Standard Model*, *Phys. Rev. D* **86** (2012) 093014 [[arXiv:1207.4599](#)] [[INSPIRE](#)].
- [23] T. Plehn and M. Rauch, *Higgs couplings after the discovery*, *Europhys. Lett.* **100** (2012) 11002 [[arXiv:1207.6108](#)] [[INSPIRE](#)].
- [24] A. Djouadi, *Precision Higgs coupling measurements at the LHC through ratios of production cross sections*, *Eur. Phys. J. C* **73** (2013) 2498 [[arXiv:1208.3436](#)] [[INSPIRE](#)].
- [25] B. Batell, S. Gori and L.-T. Wang, *Higgs couplings and precision electroweak data*, *JHEP* **01** (2013) 139 [[arXiv:1209.6382](#)] [[INSPIRE](#)].
- [26] G. Moreau, *Constraining extra-fermion(s) from the Higgs boson data*, *Phys. Rev. D* **87** (2013) 015027 [[arXiv:1210.3977](#)] [[INSPIRE](#)].
- [27] G. Cacciapaglia, A. Deandrea, G.D. La Rochelle and J.-B. Flament, *Higgs couplings beyond the Standard Model*, *JHEP* **03** (2013) 029 [[arXiv:1210.8120](#)] [[INSPIRE](#)].
- [28] A. Azatov and J. Galloway, *Electroweak symmetry breaking and the Higgs boson: confronting theories at colliders*, *Int. J. Mod. Phys. A* **28** (2013) 1330004 [[arXiv:1212.1380](#)] [[INSPIRE](#)].
- [29] E. Masso and V. Sanz, *Limits on anomalous couplings of the Higgs to electroweak gauge bosons from LEP and LHC*, *Phys. Rev. D* **87** (2013) 033001 [[arXiv:1211.1320](#)] [[INSPIRE](#)].
- [30] G. Passarino, *NLO inspired effective Lagrangians for Higgs physics*, *Nucl. Phys. B* **868** (2013) 416 [[arXiv:1209.5538](#)] [[INSPIRE](#)].
- [31] T. Corbett, O.J.P. Eboli, J. Gonzalez-Fraile and M.C. Gonzalez-Garcia, *Robust determination of the Higgs couplings: power to the data*, *Phys. Rev. D* **87** (2013) 015022 [[arXiv:1211.4580](#)] [[INSPIRE](#)].
- [32] A. Falkowski, F. Riva and A. Urbano, *Higgs at last*, *JHEP* **11** (2013) 111 [[arXiv:1303.1812](#)] [[INSPIRE](#)].
- [33] P.P. Giardino, K. Kannike, I. Masina, M. Raidal and A. Strumia, *The universal Higgs fit*, *JHEP* **05** (2014) 046 [[arXiv:1303.3570](#)] [[INSPIRE](#)].
- [34] J. Ellis and T. You, *Updated global analysis of Higgs couplings*, *JHEP* **06** (2013) 103 [[arXiv:1303.3879](#)] [[INSPIRE](#)].
- [35] A. Djouadi and G. Moreau, *The couplings of the Higgs boson and its CP properties from fits of the signal strengths and their ratios at the 7 + 8 TeV LHC*, *Eur. Phys. J. C* **73** (2013) 2512 [[arXiv:1303.6591](#)] [[INSPIRE](#)].

- [36] R. Contino, M. Ghezzi, C. Grojean, M. Muhlleitner and M. Spira, *Effective Lagrangian for a light Higgs-like scalar*, *JHEP* **07** (2013) 035 [[arXiv:1303.3876](#)] [[INSPIRE](#)].
- [37] B. Dumont, S. Fichet and G. von Gersdorff, *A Bayesian view of the Higgs sector with higher dimensional operators*, *JHEP* **07** (2013) 065 [[arXiv:1304.3369](#)] [[INSPIRE](#)].
- [38] J. Elias-Miro, J.R. Espinosa, E. Masso and A. Pomarol, *Higgs windows to new physics through $D = 6$ operators: constraints and one-loop anomalous dimensions*, *JHEP* **11** (2013) 066 [[arXiv:1308.1879](#)] [[INSPIRE](#)].
- [39] D. López-Val, T. Plehn and M. Rauch, *Measuring extended Higgs sectors as a consistent free couplings model*, *JHEP* **10** (2013) 134 [[arXiv:1308.1979](#)] [[INSPIRE](#)].
- [40] E.E. Jenkins, A.V. Manohar and M. Trott, *Renormalization group evolution of the Standard Model dimension six operators I: formalism and λ dependence*, *JHEP* **10** (2013) 087 [[arXiv:1308.2627](#)] [[INSPIRE](#)].
- [41] A. Pomarol and F. Riva, *Towards the ultimate SM fit to close in on Higgs physics*, *JHEP* **01** (2014) 151 [[arXiv:1308.2803](#)] [[INSPIRE](#)].
- [42] S. Banerjee, S. Mukhopadhyay and B. Mukhopadhyaya, *Higher dimensional operators and LHC Higgs data: the role of modified kinematics*, *Phys. Rev. D* **89** (2014) 053010 [[arXiv:1308.4860](#)] [[INSPIRE](#)].
- [43] A. Alloul, B. Fuks and V. Sanz, *Phenomenology of the Higgs effective Lagrangian via FEYNRULES*, *JHEP* **04** (2014) 110 [[arXiv:1310.5150](#)] [[INSPIRE](#)].
- [44] C. Englert et al., *Precision measurements of Higgs couplings: implications for new physics scales*, *J. Phys. G* **41** (2014) 113001 [[arXiv:1403.7191](#)] [[INSPIRE](#)].
- [45] J. Bagger et al., *The strongly interacting WW system: gold plated modes*, *Phys. Rev. D* **49** (1994) 1246 [[hep-ph/9306256](#)] [[INSPIRE](#)].
- [46] V. Koulovassilopoulos and R.S. Chivukula, *The phenomenology of a nonstandard Higgs boson in $W_L W_L$ scattering*, *Phys. Rev. D* **50** (1994) 3218 [[hep-ph/9312317](#)] [[INSPIRE](#)].
- [47] C.P. Burgess, J. Matias and M. Pospelov, *A Higgs or not a Higgs? What to do if you discover a new scalar particle*, *Int. J. Mod. Phys. A* **17** (2002) 1841 [[hep-ph/9912459](#)] [[INSPIRE](#)].
- [48] B. Grinstein and M. Trott, *A Higgs-Higgs bound state due to new physics at a TeV*, *Phys. Rev. D* **76** (2007) 073002 [[arXiv:0704.1505](#)] [[INSPIRE](#)].
- [49] R. Contino, C. Grojean, M. Moretti, F. Piccinini and R. Rattazzi, *Strong double Higgs production at the LHC*, *JHEP* **05** (2010) 089 [[arXiv:1002.1011](#)] [[INSPIRE](#)].
- [50] A. Azatov, R. Contino and J. Galloway, *Model-independent bounds on a light Higgs*, *JHEP* **04** (2012) 127 [*Erratum ibid.* **04** (2013) 140] [[arXiv:1202.3415](#)] [[INSPIRE](#)].
- [51] R. Alonso, M.B. Gavela, L. Merlo, S. Rigolin and J. Yepes, *The effective chiral Lagrangian for a light dynamical “Higgs particle”*, *Phys. Lett. B* **722** (2013) 330 [*Erratum ibid.* **B 726** (2013) 926] [[arXiv:1212.3305](#)] [[INSPIRE](#)].
- [52] R. Alonso, M.B. Gavela, L. Merlo, S. Rigolin and J. Yepes, *Flavor with a light dynamical “Higgs particle”*, *Phys. Rev. D* **87** (2013) 055019 [[arXiv:1212.3307](#)] [[INSPIRE](#)].
- [53] G. Buchalla, O. Catà and C. Krause, *Complete electroweak chiral Lagrangian with a light Higgs at NLO*, *Nucl. Phys. B* **880** (2014) 552 [[arXiv:1307.5017](#)] [[INSPIRE](#)].

- [54] I. Brivio et al., *Disentangling a dynamical Higgs*, *JHEP* **03** (2014) 024 [[arXiv:1311.1823](#)] [[INSPIRE](#)].
- [55] I. Brivio et al., *Higgs ultraviolet softening*, [arXiv:1405.5412](#) [[INSPIRE](#)].
- [56] J.R. Dell’Aquila and C.A. Nelson, *P or CP determination by sequential decays: $V_1 V_2$ modes with decays into $\bar{\ell}_A \ell_B$ and/or $\bar{q}_A q_B$* , *Phys. Rev. D* **33** (1986) 80 [[INSPIRE](#)].
- [57] J.R. Dell’Aquila and C.A. Nelson, *Distinguishing a spin-0 technipion and an elementary Higgs boson: $V_1 V_2$ modes with decays into $\bar{\ell}_A \ell_B$ and/or $\bar{q}_A q_B$* , *Phys. Rev. D* **33** (1986) 93 [[INSPIRE](#)].
- [58] J.R. Dell’Aquila and C.A. Nelson, *Simple tests for CP or P violation by sequential decays: $V_1 V_2$ modes with decays into $\bar{\ell}_A \ell_B$ and/or $\bar{q}_A q_B$* , *Phys. Rev. D* **33** (1986) 101 [[INSPIRE](#)].
- [59] A. Soni and R.M. Xu, *Probing CP-violation via Higgs decays to four leptons*, *Phys. Rev. D* **48** (1993) 5259 [[hep-ph/9301225](#)] [[INSPIRE](#)].
- [60] D. Chang, W.-Y. Keung and I. Phillips, *CP odd correlation in the decay of neutral Higgs boson into ZZ , $W^+ W^-$, or $t\bar{t}$* , *Phys. Rev. D* **48** (1993) 3225 [[hep-ph/9303226](#)] [[INSPIRE](#)].
- [61] T. Arens and L.M. Sehgal, *Energy spectra and energy correlations in the decay $H \rightarrow ZZ \rightarrow \mu^+ \mu^- \mu^+ \mu^-$* , *Z. Phys. C* **66** (1995) 89 [[hep-ph/9409396](#)] [[INSPIRE](#)].
- [62] S.Y. Choi, D.J. Miller, M.M. Muhlleitner and P.M. Zerwas, *Identifying the Higgs spin and parity in decays to Z pairs*, *Phys. Lett. B* **553** (2003) 61 [[hep-ph/0210077](#)] [[INSPIRE](#)].
- [63] C.P. Buszello, I. Fleck, P. Marquard and J.J. van der Bij, *Prospective analysis of spin- and CP-sensitive variables in $H \rightarrow ZZ \rightarrow \ell_1^+ \ell_1^- \ell_2^+ \ell_2^-$ at the LHC*, *Eur. Phys. J. C* **32** (2004) 209 [[hep-ph/0212396](#)] [[INSPIRE](#)].
- [64] R.M. Godbole, D.J. Miller and M.M. Muhlleitner, *Aspects of CP-violation in the HZZ coupling at the LHC*, *JHEP* **12** (2007) 031 [[arXiv:0708.0458](#)] [[INSPIRE](#)].
- [65] Q.-H. Cao, C.B. Jackson, W.-Y. Keung, I. Low and J. Shu, *The Higgs mechanism and loop-induced decays of a scalar into two Z bosons*, *Phys. Rev. D* **81** (2010) 015010 [[arXiv:0911.3398](#)] [[INSPIRE](#)].
- [66] Y. Gao et al., *Spin determination of single-produced resonances at hadron colliders*, *Phys. Rev. D* **81** (2010) 075022 [[arXiv:1001.3396](#)] [[INSPIRE](#)].
- [67] A. De Rujula, J. Lykken, M. Pierini, C. Rogan and M. Spiropulu, *Higgs look-alikes at the LHC*, *Phys. Rev. D* **82** (2010) 013003 [[arXiv:1001.5300](#)] [[INSPIRE](#)].
- [68] T. Plehn, D.L. Rainwater and D. Zeppenfeld, *Determining the structure of Higgs couplings at the LHC*, *Phys. Rev. Lett.* **88** (2002) 051801 [[hep-ph/0105325](#)] [[INSPIRE](#)].
- [69] C.P. Buszello and P. Marquard, *Determination of spin and CP of the Higgs boson from WBF*, [hep-ph/0603209](#) [[INSPIRE](#)].
- [70] V. Hankele, G. Klamke, D. Zeppenfeld and T. Figy, *Anomalous Higgs boson couplings in vector boson fusion at the CERN LHC*, *Phys. Rev. D* **74** (2006) 095001 [[hep-ph/0609075](#)] [[INSPIRE](#)].
- [71] G. Klamke and D. Zeppenfeld, *Higgs plus two jet production via gluon fusion as a signal at the CERN LHC*, *JHEP* **04** (2007) 052 [[hep-ph/0703202](#)] [[INSPIRE](#)].
- [72] C. Englert, M. Spannowsky and M. Takeuchi, *Measuring Higgs CP and couplings with hadronic event shapes*, *JHEP* **06** (2012) 108 [[arXiv:1203.5788](#)] [[INSPIRE](#)].

- [73] K. Odagiri, *On azimuthal spin correlations in Higgs plus jet events at LHC*, *JHEP* **03** (2003) 009 [[hep-ph/0212215](#)] [[INSPIRE](#)].
- [74] V. Del Duca et al., *Monte Carlo studies of the jet activity in Higgs + 2 jet events*, *JHEP* **10** (2006) 016 [[hep-ph/0608158](#)] [[INSPIRE](#)].
- [75] J.R. Andersen, K. Arnold and D. Zeppenfeld, *Azimuthal angle correlations for Higgs boson plus multi-jet events*, *JHEP* **06** (2010) 091 [[arXiv:1001.3822](#)] [[INSPIRE](#)].
- [76] C. Englert, D. Goncalves-Netto, K. Mawatari and T. Plehn, *Higgs quantum numbers in weak boson fusion*, *JHEP* **01** (2013) 148 [[arXiv:1212.0843](#)] [[INSPIRE](#)].
- [77] A. Djouadi, R.M. Godbole, B. Mellado and K. Mohan, *Probing the spin-parity of the Higgs boson via jet kinematics in vector boson fusion*, *Phys. Lett. B* **723** (2013) 307 [[arXiv:1301.4965](#)] [[INSPIRE](#)].
- [78] M.J. Dolan, P. Harris, M. Jankowiak and M. Spannowsky, *Constraining CP-violating Higgs sectors at the LHC using gluon fusion*, [arXiv:1406.3322](#) [[INSPIRE](#)].
- [79] N.D. Christensen, T. Han and Y. Li, *Testing CP-violation in ZZH interactions at the LHC*, *Phys. Lett. B* **693** (2010) 28 [[arXiv:1005.5393](#)] [[INSPIRE](#)].
- [80] N. Desai, D.K. Ghosh and B. Mukhopadhyaya, *CP-violating HWW couplings at the Large Hadron Collider*, *Phys. Rev. D* **83** (2011) 113004 [[arXiv:1104.3327](#)] [[INSPIRE](#)].
- [81] J. Ellis, D.S. Hwang, V. Sanz and T. You, *A fast track towards the ‘Higgs’ spin and parity*, *JHEP* **11** (2012) 134 [[arXiv:1208.6002](#)] [[INSPIRE](#)].
- [82] R. Godbole, D.J. Miller, K. Mohan and C.D. White, *Boosting Higgs CP properties via VH production at the Large Hadron Collider*, *Phys. Lett. B* **730** (2014) 275 [[arXiv:1306.2573](#)] [[INSPIRE](#)].
- [83] C. Delaunay, G. Perez, H. de Sandes and W. Skiba, *Higgs up-down CP asymmetry at the LHC*, *Phys. Rev. D* **89** (2014) 035004 [[arXiv:1308.4930](#)] [[INSPIRE](#)].
- [84] M.B. Voloshin, *CP violation in Higgs diphoton decay in models with vectorlike heavy fermions*, *Phys. Rev. D* **86** (2012) 093016 [[arXiv:1208.4303](#)] [[INSPIRE](#)].
- [85] A.Y. Korchin and V.A. Kovalchuk, *Polarization effects in the Higgs boson decay to γZ and test of CP and CPT symmetries*, *Phys. Rev. D* **88** (2013) 036009 [[arXiv:1303.0365](#)] [[INSPIRE](#)].
- [86] F. Bishara et al., *Probing CP-violation in $h \rightarrow \gamma\gamma$ with converted photons*, *JHEP* **04** (2014) 084 [[arXiv:1312.2955](#)] [[INSPIRE](#)].
- [87] Y. Chen, A. Falkowski, I. Low and R. Vega-Morales, *New observables for CP-violation in Higgs decays*, [arXiv:1405.6723](#) [[INSPIRE](#)].
- [88] A. Freitas and P. Schwaller, *Higgs CP properties from early LHC data*, *Phys. Rev. D* **87** (2013) 055014 [[arXiv:1211.1980](#)] [[INSPIRE](#)].
- [89] H. Belusca-Maito, *Effective Higgs Lagrangian and constraints on Higgs couplings*, [arXiv:1404.5343](#) [[INSPIRE](#)].
- [90] J. Shu and Y. Zhang, *Impact of a CP-violating Higgs sector: from LHC to baryogenesis*, *Phys. Rev. Lett.* **111** (2013) 091801 [[arXiv:1304.0773](#)] [[INSPIRE](#)].
- [91] K. Cheung, J.S. Lee and P.-Y. Tseng, *Higgs precision (Higgcision) era begins*, *JHEP* **05** (2013) 134 [[arXiv:1302.3794](#)] [[INSPIRE](#)].

- [92] T. Appelquist and C.W. Bernard, *Strongly interacting Higgs bosons*, *Phys. Rev. D* **22** (1980) 200 [INSPIRE].
- [93] A.C. Longhitano, *Heavy Higgs bosons in the Weinberg-Salam model*, *Phys. Rev. D* **22** (1980) 1166 [INSPIRE].
- [94] A.C. Longhitano, *Low-energy impact of a heavy Higgs boson sector*, *Nucl. Phys. B* **188** (1981) 118 [INSPIRE].
- [95] T. Appelquist and G.-H. Wu, *The electroweak chiral Lagrangian and new precision measurements*, *Phys. Rev. D* **48** (1993) 3235 [hep-ph/9304240] [INSPIRE].
- [96] H. Georgi, D.B. Kaplan and L. Randall, *Manifesting the invisible axion at low-energies*, *Phys. Lett. B* **169** (1986) 73 [INSPIRE].
- [97] K. Hagiwara, R.D. Peccei, D. Zeppenfeld and K. Hikasa, *Probing the weak boson sector in $e^+e^- \rightarrow W^+W^-$* , *Nucl. Phys. B* **282** (1987) 253 [INSPIRE].
- [98] T. Appelquist, M. Piai and R. Shrock, *Lepton dipole moments in extended technicolor models*, *Phys. Lett. B* **593** (2004) 175 [hep-ph/0401114] [INSPIRE].
- [99] W.J. Marciano and A. Queijeiro, *Bound on the W boson electric dipole moment*, *Phys. Rev. D* **33** (1986) 3449 [INSPIRE].
- [100] ACME collaboration, J. Baron et al., *Order of magnitude smaller limit on the electric dipole moment of the electron*, *Science* **343** (2014) 269 [arXiv:1310.7534] [INSPIRE].
- [101] C.A. Baker et al., *An improved experimental limit on the electric dipole moment of the neutron*, *Phys. Rev. Lett.* **97** (2006) 131801 [hep-ex/0602020] [INSPIRE].
- [102] S. Dawson, S.K. Gupta and G. Valencia, *CP violating anomalous couplings in $W\gamma$ and $Z\gamma$ production at the LHC*, *Phys. Rev. D* **88** (2013) 035008 [arXiv:1304.3514] [INSPIRE].
- [103] OPAL collaboration, G. Abbiendi et al., *Measurement of W boson polarizations and CP -violating triple gauge couplings from W^+W^- production at LEP*, *Eur. Phys. J. C* **19** (2001) 229 [hep-ex/0009021] [INSPIRE].
- [104] DELPHI collaboration, J. Abdallah et al., *Study of W boson polarisations and triple gauge boson couplings in the reaction $e^+e^- \rightarrow W^+W^-$ at LEP 2*, *Eur. Phys. J. C* **54** (2008) 345 [arXiv:0801.1235] [INSPIRE].
- [105] ALEPH collaboration, S. Schael et al., *Improved measurement of the triple gauge-boson couplings γWW and ZWW in e^+e^- collisions*, *Phys. Lett. B* **614** (2005) 7 [INSPIRE].
- [106] PARTICLE DATA GROUP collaboration, J. Beringer et al., *Review of particle physics (RPP)*, *Phys. Rev. D* **86** (2012) 010001 [INSPIRE].
- [107] O.J.P. Eboli, J. Gonzalez-Fraile and M.C. Gonzalez-Garcia, *Scrutinizing the ZW^+W^- vertex at the Large Hadron Collider at 7 TeV*, *Phys. Lett. B* **692** (2010) 20 [arXiv:1006.3562] [INSPIRE].
- [108] ATLAS collaboration, *Measurement of WZ production in proton-proton collisions at $\sqrt{s} = 7$ TeV with the ATLAS detector*, *Eur. Phys. J. C* **72** (2012) 2173 [arXiv:1208.1390] [INSPIRE].
- [109] N.D. Christensen and C. Duhr, *FeynRules — Feynman rules made easy*, *Comput. Phys. Commun.* **180** (2009) 1614 [arXiv:0806.4194] [INSPIRE].
- [110] J. Alwall, M. Herquet, F. Maltoni, O. Mattelaer and T. Stelzer, *MadGraph 5: going beyond*, *JHEP* **06** (2011) 128 [arXiv:1106.0522] [INSPIRE].

- [111] T. Sjöstrand, S. Mrenna and P.Z. Skands, *PYTHIA 6.4 physics and manual*, *JHEP* **05** (2006) 026 [[hep-ph/0603175](#)] [[INSPIRE](#)].
- [112] J. Conway, *PGS4 — Pretty Good Simulation of high energy collisions webpage*, <http://www.physics.ucdavis.edu/~conway/research/software/pgs/pgs4-general.htm>.
- [113] S. Dawson, X.-G. He and G. Valencia, *CP violation in $W\gamma$ and $Z\gamma$ production*, *Phys. Lett. B* **390** (1997) 431 [[hep-ph/9609523](#)] [[INSPIRE](#)].
- [114] J. Kumar, A. Rajaraman and J.D. Wells, *Probing CP-violation at colliders through interference effects in diboson production and decay*, *Phys. Rev. D* **78** (2008) 035014 [[arXiv:0801.2891](#)] [[INSPIRE](#)].
- [115] T. Han and Y. Li, *Genuine CP-odd observables at the LHC*, *Phys. Lett. B* **683** (2010) 278 [[arXiv:0911.2933](#)] [[INSPIRE](#)].
- [116] M. Spira, A. Djouadi, D. Graudenz and P.M. Zerwas, *Higgs boson production at the LHC*, *Nucl. Phys. B* **453** (1995) 17 [[hep-ph/9504378](#)] [[INSPIRE](#)].
- [117] D. McKeen, M. Pospelov and A. Ritz, *Modified Higgs branching ratios versus CP and lepton flavor violation*, *Phys. Rev. D* **86** (2012) 113004 [[arXiv:1208.4597](#)] [[INSPIRE](#)].
- [118] CMS collaboration, *Study of the mass and spin-parity of the Higgs boson candidate via its decays to Z boson pairs*, *Phys. Rev. Lett.* **110** (2013) 081803 [[arXiv:1212.6639](#)] [[INSPIRE](#)].
- [119] ATLAS collaboration, *Evidence for the spin-0 nature of the Higgs boson using ATLAS data*, *Phys. Lett. B* **726** (2013) 120 [[arXiv:1307.1432](#)] [[INSPIRE](#)].
- [120] ATLAS collaboration, *Measurements of the properties of the Higgs-like boson in the four lepton decay channel with the ATLAS detector using 25 fb^{-1} of proton-proton collision data*, *ATLAS-CONF-2013-013*, CERN, Geneva Switzerland (2013).
- [121] CMS collaboration, *Projected performance of an upgraded CMS detector at the LHC and HL-LHC: contribution to the Snowmass process*, [arXiv:1307.7135](#) [[INSPIRE](#)].